Μελέτη διεισδυτικότητας καρκινικών κυττάρων σε οργανοειδή προερχόμενα από καρκινοπαθείς

Πτυχιακή εργασία

Πανεπιστήμιο Μιλάνου,

Τμήμα Ιατρικής Βιοτεχνολογίας και Μεταφραστικής Ιατρικής

Νικολέτα Τσιαντούλη του Αντωνίου

Επιβλέπων καθηγητής: Massimiliano Pagani, καθηγητής Μοριακής Βιολογίας

Πανεπιστημίου Μιλάνου, Ιταλία

Μιλάνο (Ιταλία), 2023

A patient-derived 3D model of cancer cell invasiveness

Bachelor thesis

University of Milan,

Department of Medical Biotechnology and Translational Medicine

Nikoleta Tsiantouli

Supervisor: Massimiliano Pagani, Full Professor of Molecular Biology at the University of Milan (Italy)

Milan (Italy), 2023

Περίληψη

Η μετάσταση είναι μια βιολογικά πολύπλοκη διαδικασία, η οποία ευθύνεται για άνω το 90% των θανάτων που σχετίζονται με τον καρκίνο. Η καλύτερη κατανόηση των υποκείμενων μηχανισμών της είναι ζωτικής σημασίας για την ανάπτυξη πιο αποτελεσματικών θεραπευτικών στρατηγικών και τη βελτίωση των αποτελεσμάτων των ασθενών. Ένα από τα χαρακτηριστικά της μετάστασης είναι η απόκτηση φαινοτύπων απαραίτητων για την διείσδυση τους στο υποκείμενο στρώμα. Πολλές in vitro δοκιμασίες έχουν χρησιμοποιηθεί στο παρελθόν για την εξέταση αυτής της ικανότητας των κυττάρων του καρκίνου. Ωστόσο, έχουν πολλούς περιορισμούς, καθώς επικεντρώνονται κυρίως στη μετανάστευση τους, ενώ η χρήση κυτταρικών σειρών δεν επιτρέπει την αναπαράσταση του πολύπλοκου τρισδιάστατου (3D) περιβάλλοντος του όγκου. Επομένως, είναι αναγκαία η μετάβαση σε 3D in vitro δοκιμασίες, οι οποίες θα δώσουν πιο σχετικές από φυσιολογικής άποψης πληροφορίες. Γι' αυτόν τον λόγο, η συγκεκριμένη διατριβή επικεντρώνεται στην εγκαθίδρυση μιας νέας 3D in vitro δοκιμασίας για την αξιολόγηση της διεισδυτικής ικανότητας οργανοειδών από φυσιολογικό ιστό, όγκους και μεταστάσεις προερχόμενα από ασθενείς (PDOs). Η έρευνα ξεκινά με μια εκτενή ανασκόπηση της τρέχουσας βιβλιογραφίας σχετικά με τον καρκίνο και, ειδικότερα, τη μετάσταση, και εξετάζει τις συνθήκες που απαιτούνται για να αντιπροσωπευτούν καλύτερα οι πολύπλοκες διαδικασίες της in vivo διείσδυσης. Η ερευνητική διαδικασία περιλαμβάνει την καλλιέργεια των φυσιολογικών, καρκινικών και μεταστατικών οργανοειδών προερχόμενα από ασθενείς σε ένα 3D εξωκυττάριο πλέγμα, επιτρέποντας την επίδειξη σημαντικών διαφορών στην ικανότητα διείσδυσης και των μοριακών προφίλ μεταξύ των PDOs. Τα ευρήματα υπογραμμίζουν τη χρησιμότητας αυτής της νέας προσέγγισης στη μελέτη της διείσδυσης των καρκινικών κυττάρων και παρέχουν πολύτιμες πληροφορίες σχετικά με την ικανότητα αυτή που αποκτούν κατά τη διάρκεια της μετάστασης. Τελικά, η συγκεκριμένη έρευνα συμβάλλει στον αυξανόμενο όγκο γνώσης σχετιζόμενο με την διαδικασία της μετάστασης και ανοίγει τον δρόμο για την ανάπτυξη νέων θεραπευτικών στρατηγικών που στοχεύουν εξειδικευμένα τα μεταστατικά καρκινικά κύτταρα, με τελικό στόχο τη βελτίωση του ποσοστού επιβίωσης.

Abstract

Metastasis is a biologically complex multi-step process, which is responsible for more than 90% of cancer-related deaths. Better understanding of the underlying mechanisms is vital for developing more effective therapeutic strategies and having improved patient outcomes. One of the hallmarks of metastasis is the acquisition of invasive phenotypes, in order to penetrate the underlying stroma. Many in vitro assays have been used in the past to investigate this ability of cancer cells. However, they have many limitations, as they are mostly focused on migration and the usage of cells lines does not allow the recapitulation of the complex 3D environment of the tumor. Therefore, it is deemed crucial to transition to more informative physiologically relevant 3D in vitro invasion assays. For this reason, this thesis focuses on the establishment of a novel 3D in vitro assay to evaluate the invasive potential of normal, tumor and metastasis patient-derived organoids (PDOs). The research begins with an extensive review of the current literature on cancer and particularly metastasis and explores the conditions necessary to better represent the complexities of the in vivo invasion process. The setup involves culturing normal, tumor and metastasis PDOs within a three-dimensional extracellular matrix allowing the demonstration of significant differences in invasive behaviors and molecular profiles between the PDOs. The findings highlight the utility of this novel approach in studying tumor invasion and provide valuable insights into the invasive potential of metastatic cells. Ultimately, this research contributes to the growing body of knowledge surrounding cancer metastasis and paves the way for development of novel therapeutic strategies specifically targeting metastatic cancer cells, with the ultimate goal of improving survival rate.

Table of Contents

Acknowledgements

I would like to take this opportunity to express my heartfelt gratitude to all those who have been instrumental in the successful completion of this thesis. First and foremost, I extend my deepest appreciation to Professor Pagani for accepting me and providing me with this incredible opportunity to be a part of such a dynamic research environment, which has been instrumental in shaping my academic journey. A special acknowledgment goes to Roberta Bordo, my supervisor, for her unwavering patience, trust, and belief in me, especially during moments when I doubted myself. I have learned so much under her guidance and I am truly grateful for the chance to work under her mentorship. I would also like to express my sincere gratitude to Michaela Fakiola for the support she provided me with both before and during my time in the laboratory. Your encouragement, advice, and unwavering friendship have been a constant source of motivation. To my family, Antonis, Eleni, and Maria, I am immensely grateful for your unwavering support and understanding. I could not have pursued this endeavour without you by my side. I would also like to extend my heartfelt thanks to my friends from Greece, particularly Anastasis Savellos, and Milan, especially Ramveer Choudhary. Your friendship and encouragement have been a bright light during challenging times. This thesis would not have been possible without the support and guidance of the mentioned individuals and many others who have contributed in different ways. I am truly humbled and grateful for this opportunity and these experiences, which I will always carry with me throughout my research and personal journey.

1. Introduction

1.1 Colorectal Cancer (CRC)

1.1.1 Epidemiology

Colorectal cancer (CRC) is the third most diagnosed cancer and the second leading cause of cancer-related mortality globally, with an estimated number of 1.93 million new cases and 935.173 deaths in 2020 [1]. Rates of both incidence and mortality are substantially higher in men than in women, with the estimated lifetime risk of developing CRC being about 1 in 23 for men and 1 in 26 for women [2]. According to data from 2012-2018 the 5-year survival rate is about 65.1% and is strongly influenced by the cancer stage at the diagnosis, as patients with localized or regional tumour sites statistically have a better chance of surviving after five years of being diagnosed, than those with metastasis [3]. In general, colorectal cancer is most frequently diagnosed among people aged 65-74, with the median age at death being 72 years[3]. The epidemiological characteristics of CRC differ significantly between regions in the world. Almost half (49.3%) of new cases in 2020 were observed in Asia, while Europe is the second leading continent in incident rate (22.8%) [1].

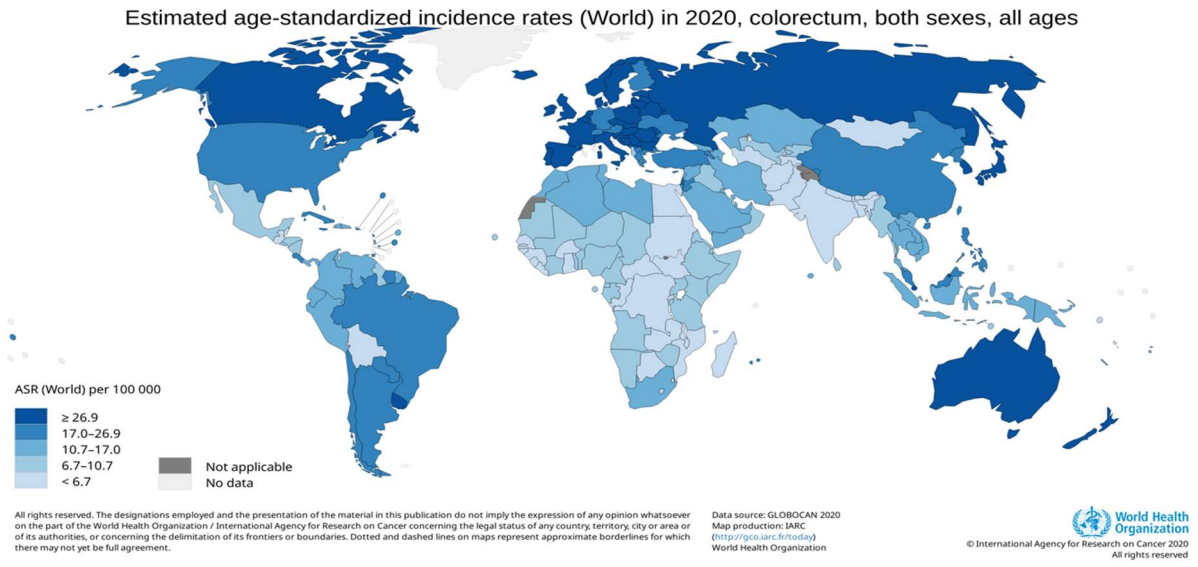

Figure 1: Incidents of colorectal cancer worldwide in 2020 for both sexes and all ages. Darker shades indicate increasing frequency. Source: Global Cancer Observatory

1.1.2 Risk Factors for Developing CRC

Many years of research have allowed the scientific community to identify modifiable risk factors, that have been associated with the occurrence of colorectal neoplasms.

Obesity and physical inactivity

Both obesity and lack of exercise are the most important behavioral factors in the development of CRC, but can also decrease the likelihood of survival. Studies have shown that increasing BMI can be linked with a statistically significant increased risk, while a meta-analysis proposed that even a 5-kg weight gain can lead to a 3% increased risk [4,5]. Generally, body weight has an immense effect on carcinogenesis and has been associated with chronic low-grade inflammation, which promotes the transcription of genes that promote metaplasia and various forms of cancer development, including CRC [6].

Diet

Diet can also play an adverse or protective role. High consumption of processed or red meat such as beef and pork, which were designated in 2015 by the International Agency for Research on Cancer (IARC) as carcinogenic or possibly carcinogenic respectively, is a major risk for colorectal cancer [5,7,8]. Several mechanisms may underlie this relationship between red meat and CRC. Heme iron in red meat can induce oxidative stress, colonocyte proliferation and the endogenous formation of N-nitroso compounds (NOCs), which are potent carcinogens in the gastrointestinal tract [9]. Meat cooked at high temperatures is also a source of other mutagens, including heterocyclic amines (HCAs) and polycyclic aromatic hydrocarbons (PAHs)[9]. On the other hand, fruits, vegetables and foods that contain calcium, fibre and Vitamin D have been shown to have a protective effect against CRC, even though the results are conflicting [7–12].

Smoking

Tobacco smoke contains more than 60 known carcinogens including heterocyclic amines, nitrosamines and polycyclic hydrocarbons and is a leading cause of preventable malignancies, including CRC. According to a meta-analysis published in 2009, smoking for more than 20 years can increase the risk of CRC and more so for those who smoked for more than 30 years. Additionally, the effects of cigarette smoking on the risk of CRC appear to be dose-related, as smokers who consumed more than 30 pack-years or more than 20 cigarettes per day, the risks of CRC increased by 34% or 46%, respectively [13]. Another recent study in mice displayed that cigarette smoking could promote colon tumorigenesis by modulating the composition of gut microbiota and inducing gut microbiota dysbiosis[14].

Alcohol

A positive dose-related association between alcoholic beverages and CRC risk has been proposed. A meta-analysis of published studies reported that moderate drinking (>1-4 drinks/day) and heavy drinking (≥4 drinks/day) were linked with a 21% and 52% increased risk for colorectal cancer respectively [15]. It has been suggested that alcohol's carcinogenic effects are partially attributed to acetaldehyde's genotoxicity, which is the main metabolite of ethanol[16] and can be modulated by polymorphisms in genes encoding aldehyde dehydrogenase 2 (ALDH2), as an enhanced risk has been associated with ALDH2 heterozygotes [17].

1.1.3 Histopathological Classification of CRC

Most colorectal cancer neoplasms usually initiate from the growth of the inner lining of the colon or rectum. These protrusions are called polyps and generally are benign, but might become malignant with time[18]. The different types of polyps are adenomatous polyps (adenomas), hyperplastic polyps and inflammatory polyps, sessile serrated polyps (SSP) and traditional serrated adenomas (TSA). The most common form (96% of CRCs) is an adenoma or polyp that originated from granular cells, which produce mucus that lubricates the inside of the colon and rectum. Only about 10% of all adenomas progress to invasive cancer (adenocarcinoma), although this depends on the size of the polyp, as the risk of cancer

increases when the polys grow larger [18,19]. Adenocarcinoma's histological subtypes include Mucinous adenocarcinoma, Signet ring cell carcinoma, Medullary carcinoma, Serrated adenocarcinoma and Micropapillary adenocarcinoma. Even though the majority of CRC tumors are adenocarcinomas, other rare variants include neuroendocrine neoplasms, lymphomas, mesenchymal tumors and melanomas, which generally have a worse prognosis[20].

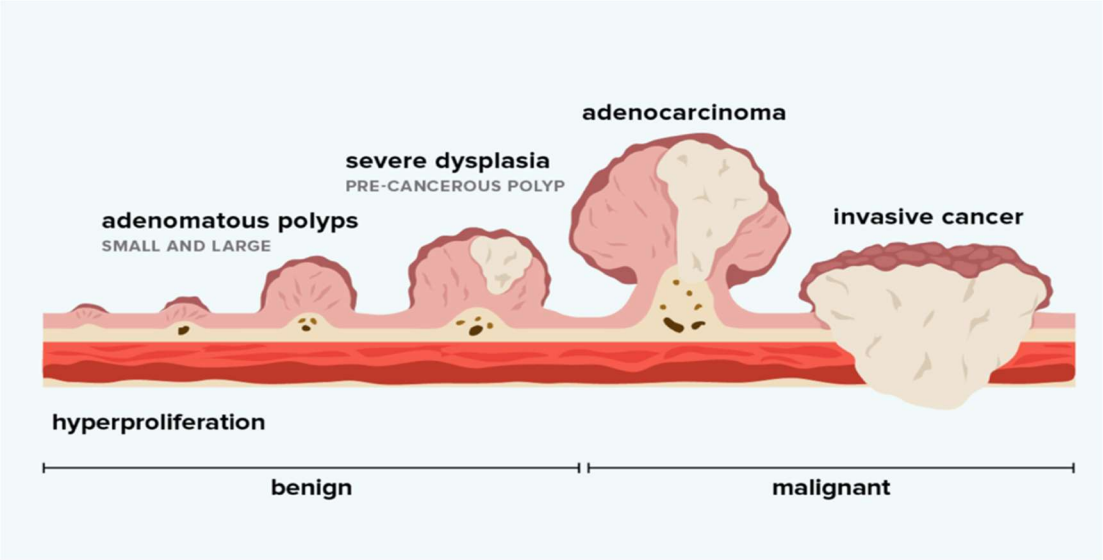

Figure 2: Figure 2: Colon polyp sizes and level risk based on polyp size. Source: Healthline

1.1.4 Genomic Instability in Colorectal Cancer

The process of colorectal carcinogenesis involves the accumulation of multiple genetic alterations, that enable the establishment of successive clones each characterized by a relative growth advantage. Apart from this growth advantage, which is often due to increased proliferation or impaired apoptosis, pre-cancerous cells also require to develop a permissive environment for the acquisition of future mutations. This is achieved by genomic instability, which is a critical hallmark for CRC transformation and regulates the neoplastic evolutionary process [21]. Three distinct pathways of genomic instability have been recognized: (1) Chromosomal Instability (CIN) pathway, (2) Microsatellite Instability (MSI), and (3) CpG Island Methylator Phenotype pathways (CIMP).

Chromosomal Instability Pathway (CIN)

This pathway represents approximately 70-85% of total CRCs and has also been referred to as the 'suppressor' pathway or 'adenocarcinoma sequence' [21,22]. CIN involves the activation of proto-oncogenes, such as K-Ras and the inactivation of at least three tumor suppression genes including Adenomatous Polyposis Coli (APC), located in chromosome region 5q21, p53, located in chromosome region 17p13 and loss of heterozygosity for the long arm of chromosome 18 (18q LOH). Other crucial mutations have been identified in genes, such as TGFBR and PIK3CA. Both sporadic and hereditary CRC is majorly influenced by the APC/Wnt/β-catenin pathway. Most of the APC mutations are either frameshift or nonsense mutations and result in a truncated protein [22]. APC inactivation leads to the accumulation of β-catenin, retention of stem cell phenotype in the colonic crypts and thereby formation of a polyp. Familial Adenomatous Polyposis (FAP) is an example of the corruption of this pathway [22]. While APC mutations occur specifically in adenomas, K-Ras mutations are present in both adenomas and hyperplastic polyps. Activating mutations in the K-Ras gene, which encodes for a GTP-binding protein, are found in 35-42% of CRCs and are considered molecular shortcuts to developing advanced adenomas [21]. Finally, the acquisition of mutations on the TP53 gene accompanies this transition from pre-invasive benign lesion to invasive disease [21].

Microsatellite Instability (MSI)

About 20% of CRCs exhibit the otherwise called 'mutator' phenotype, in which the mismatch repair system (MMR) fails to repair the errors that are missed by the proofreading function of DNA polymerase. This results in detectable differences in the number of copies found in the repeat sequences (microsatellites). 'Microsatellite high' (MSI-H) is defined as the presence of instability in more than 40% of five specified microsatellite sites (two mononucleotide and three dinucleotide microsatellites) and interestingly are associated with a good clinical outcome. MSI-H occur in Lynch syndrome, which makes up 3-5% of all colorectal cancers and is caused by germline mutations in one of the several MMR genes. In 80% of cases, individuals with germline loss of DNA mismatch repair usually develop CRC by the age of 40[22].

CpG Island Methylator Phenotype (CIMP)

During carcinogenesis, the biological impact of epigenetic silencing of gene transcription through CpG island methylation is equivalent to the acquisition of inactivating mutations[21]. MSI-H cancers, which were previously mentioned, occur sporadically following the methylation of MLH1, which is one of the seven MMR proteins. CIMP+ cancers are also characterized by a signature mutation in the protein BRAF, a critical member of the RAS-RAF-MEK-ERK signalling pathway which is involved in anoikis. Failure of this type of apoptosis plays a major role in the development of hyperplastic polyps[21].

1.1.5 Molecular subtypes

Colorectal cancer is characterized by high inter-patient and intra-tumor heterogeneity, which directly influences tumor aggressiveness, resistance to therapy and patient prognosis and is dependent on its molecular subtype[23]. Molecular classification provides valuable insight into the aetiology and characteristics of cancer, ultimately leading to better understanding and improved therapies[24]. In 2015 an analysis of 4151 CRC samples led to the establishment of a robust classification system, the Consensus Molecular Subtype (CMS) system. This classification consists of four subtypes:

I. CMS1 (MSI Immune)

   This particular subtype accounts for 14% of total CRC tumors and displays a poor prognosis. It is characterized by a hypermethylation status, low Somatic Copy Number Alterations (SCNAs), MSI high and CIMP+ phenotype with frequent BRAF mutations and immune infiltration.

II. CMS2 (Canonical)

   These represent 37% of all tumor subtypes, display a strong upregulation of WNT and MYC pathways and are SCNA-high.

III. CMS3 (Metabolic)

   This subtype is characterized by enrichment in multiple metabolic signatures, KRAS-activating mutations and exhibit mixed MSI status, SCNA low and CIMP low profile.

IV. CMS4 (Mesenchymal)

These SCNA-high tumors show an upregulation in genes implicated in Epithelial t Mesenchymal Transition (EMT), activation of Transforming Growth Factor β (TGF-β), angiogenesis, matrix remodeling pathways and inflammatory-related system[25].

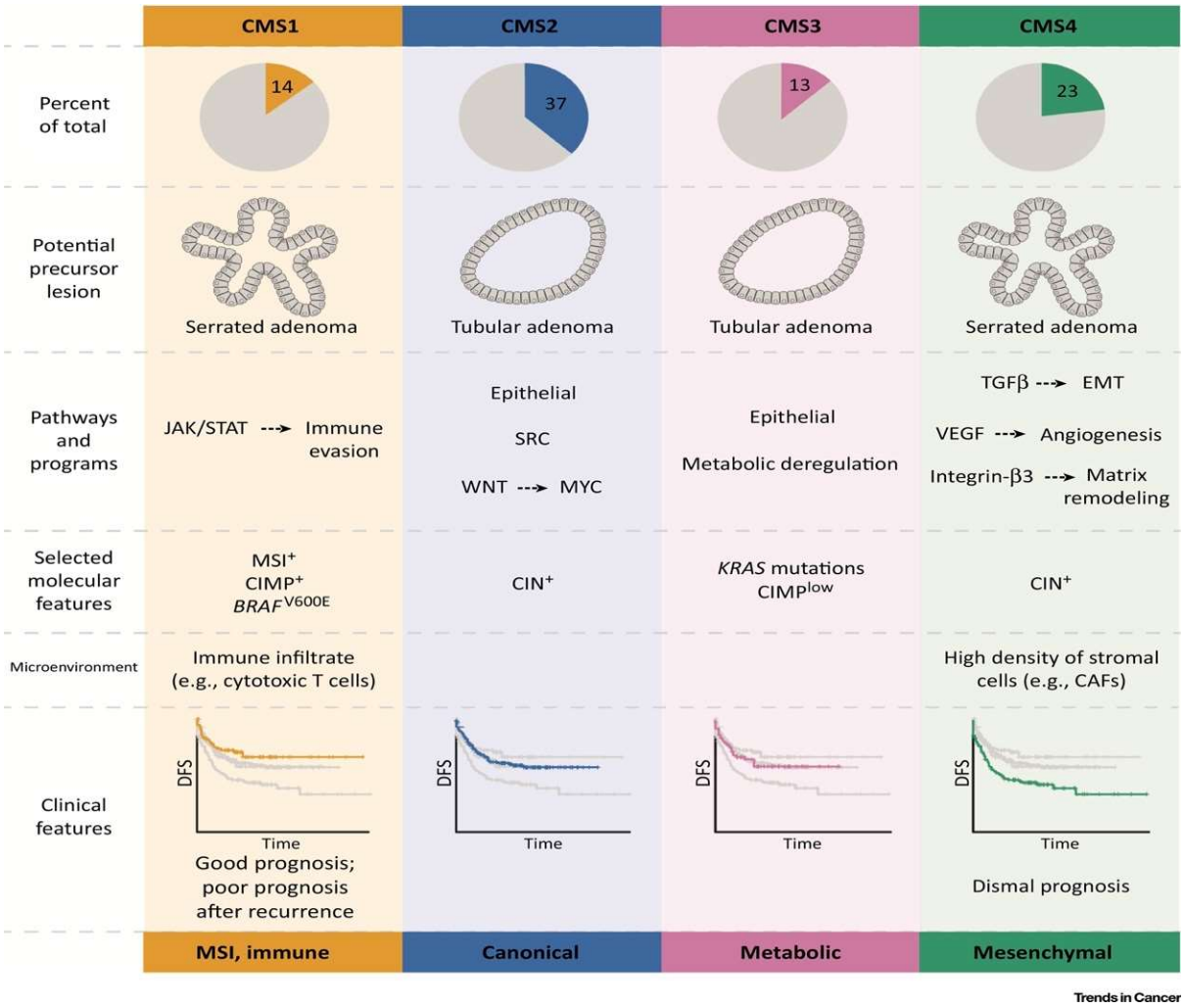

Figure 3: The Consensus Molecular Subtypes of Colorectal Cancer [26]

1.2 Metastasis

Cancer metastasis is the spread of cancer cells and the development of secondary tumors to a part of the body, that is far from and no longer connected to the original primary tumor site. This process entails a dynamic interplay of both inherent characteristics of tumors and

interactions with the multiple microenvironments and it is thought to be the ultimate expression of a neoplastic cell's progression towards autonomy from its host. Each cancer cell needs to acquire certain characteristics, that distinguish them genetically, biochemically and behaviorally from the remaining cells at the primary tumor and enable them to successfully complete a series of steps in the metastatic cascade[27]. Metastasis initiates well in advance of the detectability of the tumor, as the primary tumor before the arrival of any carcinoma cell selectively prepares the host microenvironment, termed as 'pre-metastatic niche' to be supportive of the establishment and tumor growth [27]. This multiple-step procedure involves the release of secretory factors and extracellular vesicles, that induce vascular leakage, ECM remodeling and immunosuppression[27,28]. Cells may be 'motivated' to disseminate due to limited nutrients or oxygen in the primary tumor site. The metastatic capability is thought to be controlled by several pro-metastatic genes, that are regulated by the hypoxia-inducible factor (HIF-1) [27]. In order for cells to gain motility and initiate the invasion, they need to acquire mesenchymal characteristics through the Epithelial to Mesenchymal Transition (EMT). The EMT program is a spectrum of transitional stagers between epithelial and mesenchymal phenotypes, in which the epithelial immotile polarized cells lose their apical-basal organization and acquire a fibroblast-like shape. Fundamental changes are also observed at different genetic, epigenetic, transcriptional and post-transcriptional levels in response to signals from the microenvironment, contributing to plasticity [27–29]. At the transcriptional level, several transcriptional factors including zinc-finger proteins (SNAI1/2 and ZEB1/2) and basic helix-loop-helix proteins (TWIST1/2) are involved in the activation and regulation of EMT, while molecularly it is mainly characterized by loss of epithelial-specific E-cadherin, cytokeratins and occludins and upregulation of N-cadherin, fibronectin, laminin and vimentin [29]. EMT is governed by signalling pathways and growth factors, such a TGF-β, Epidermal Growth Factor (EGF) or Platelet-derived Growth Factor (PDGF), which are secreted by the tumor microenvironment [28,29]. This process is mainly observed in cells at the invasive front, where there is an interaction with the stromal cells and the extracellular matrix or the microenvironment [30]. Upon seeding at the secondary metastatic sites, can either cells revert to their epithelial phenotype through the process of Mesenchymal to Epithelial Transition (MET), in order to resume their proliferative capacity, trans-differentiate into new distinct cell states, or even demonstrate deformability [31]. However, the contribution of EMT to the metastatic process and its effect on stemness has been controversial [30]. Malignant cells, in

order to breach the basement membrane and infiltrate the surrounding stroma, remodel the extracellular matrix (ECM) through the recruitment of degrative enzymes, such as matrix metalloproteinases (MMPs) or cathepsins, produced by either tumor cells or tumor-associated cells [27]. Generally, ECM remodeling is a normal process, that occurs during wound healing and tissue repair and has been co-opted by tumors. Even though millions of tumor cells vasculature daily, only less than 0.01% will successfully colonize the secondary sites. In the bloodstream, the circulating tumor cells (CTCs) have to endure a harsh environment, because of the velocity-induced shear forces and the presence of the immune cells [27–29,32]. Through interaction with platelets and down-regulation of antigens, CTCs are able to evade immune insults [27,28]. Following circulation, malignant cells extravasate at the target site and colonize the tissue. The successful establishment of a colony depends significantly on the interaction with the microenvironment or 'soil' of the remote tissue [32]. Some disseminated tumor cells (DTCs) may go through dormancy, representing a balance between proliferation and apoptosis [27,32], while others might never proliferate to form a macroscopic lesion [27]. Elimination of DTCs can occur due to oxidative stress, lack of nutrients or growth factors [31]. DTCs also encounter again the tissue-resident immunosurveillant macrophages and natural killer (NK) cells, which further recruit more immune cells. However, have developed adaptive mechanisms that enable them to hijack and reprogram the immune microenvironment. These include restricting antigen recognition, upregulating receptors that block the adaptive immune system and secreting immunomodulatory cytokines, extracellular vesicles and growth factors [31].

Recently, EMP1 (Epithelial Membrane Protein 1) has been identified as a marker of a unique tumor cell population responsible for metastasis recurrence, named high relapse cells (HRCs) [33]. Both EMP1 and L1CAM, another novel marker, which is expressed during wound-healing and tissue regeneration, are highly expressed by tumor cells at the invasion fronts, The expression of Lgr5 seems to be lost and reacquired during metastatic outgrowth [31,33].

Even though metastasis constitutes the primary cause of death for >90% of patients with cancer [28], it remains poorly understood and is associated with a terminal label.

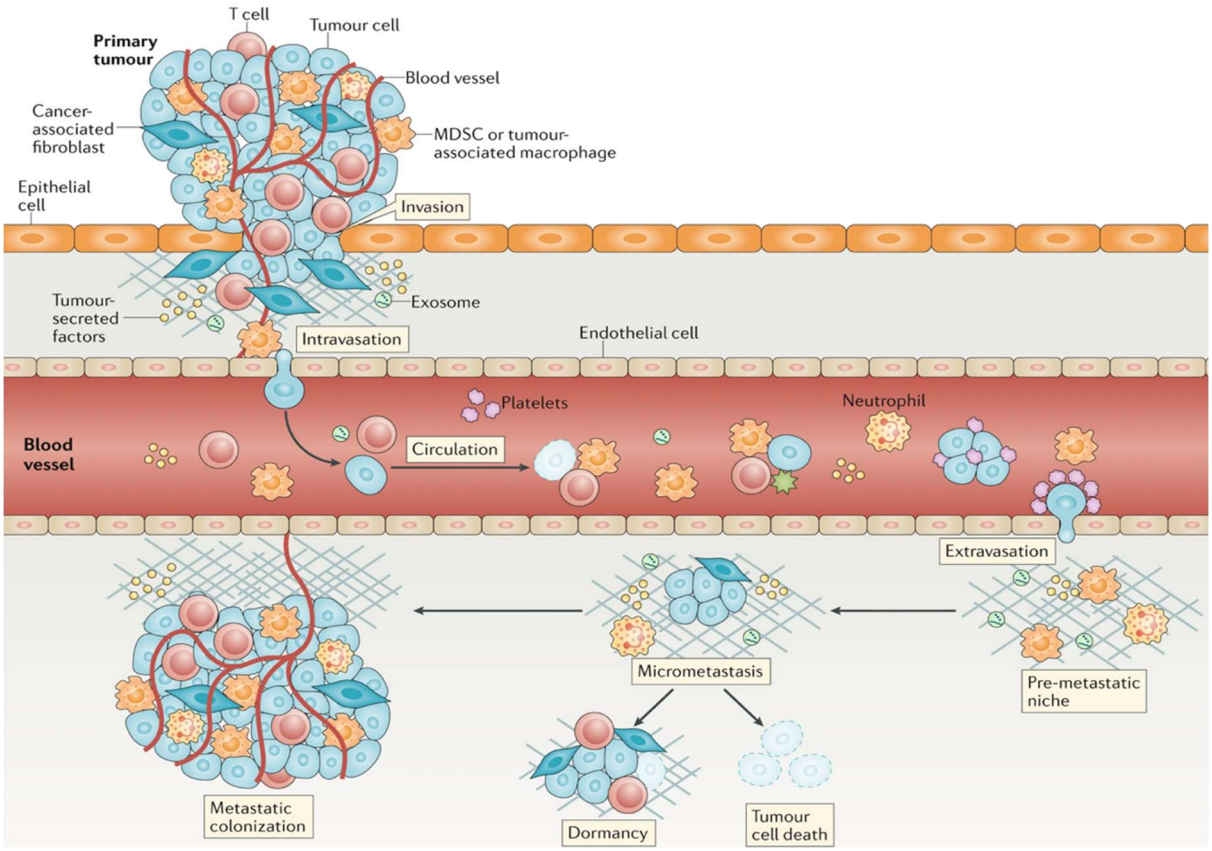

Figure 4: The multistep process of metastasis and the different cell types that are involved. Source: Chen HC. Boyden Chamber Assay. In: Cell Migration. Humana Press; :015-022

1.2.1 CRC metastasis

About 20% of patients with CRC have already developed metastasis at the time of the primary diagnosis. The most common sites of metastasis in colorectal cancer include the liver and the thorax, while the peritoneum and the bone can be usual metastatic sites too [34]. Brain metastasis (BM) occurs less frequently, with an average incidence of 2.1 %, but in the case of BM development, the prognosis is poor and late, as patients are asymptomatic [35].

1.2.2 In vitro invasion assays

Many reliable in vitro techniques to evaluate invasion properties have been developed and used over the years. The wound healing assay is one of the earliest methods developed to

investigate directional cell migration in vitro. This method involves creating a 'wound' in a cell monolayer, capturing images at the start and regularly during cell migration close to the wound and comparing the images to measure the cells' migration rate [36]. Another method commonly used is the Boyden chamber assay, also known as trans-well migration assay. Typically, cells are seeded in the upper compartment and allowed to migrate through the membrane pores into the lower chamber. After incubation, the membrane is fixed and stained, and the number of cells, that have migrated to the lower chamber is determined [37]. Other methods include the transwell, Matrigel and collagen invasive assay. However, these assays are used for monolayers and do provide important insight into the behaviour of cells in more physiologically relevant environments. They are mainly focused on migration and they do not represent the interactions between cells and the matrix. In recent years, new 3D invasion assays have been described as a useful tool to evaluate cell invasion in a more realistic setting. The 3D tumor spheroid invasion is an example of a standardized and rapid invasion system, in which a basement membrane-like matrix (BMM) is added to each well, that contains a spheroid. The BMM provides a semi-solid matrix and facilitates tumor cell invasion from the spheroid body. Compared to other invasion assays, this method provides the main advantage of organizing tumor cells into a 3D structure that mimics a micro-metastasis or a tumor micro-region, while the tumor spheroids are highly reproducible in size [38].

1.3 Organoids

For decades, cancer cell lines have been used as a low-cost, easy to use and high reproducibility human cancer model. However, they display some important drawbacks. For instance, these 2D monolayer models can be constructed only from a limited number of cancer subtypes, do not recapitulate the tumour cell microenvironment and its heterogeneity and also lack dimensionality. Other limitations include the absence of normal tissue-derived control lines and the lack of stromal compartments [39–41]. Patient-derived tumour xenografts (PDTXs), which are generated through subcutaneously or orthotopically transplantation of freshly obtained patient material into immunodeficient mice, are also commonly used in cancer research. Even though PDTXs retain the ability to mimic the

tumour's morphological and molecular characteristics during the passage, their generation takes more than 4 months, they are expensive and labour-intensive and most importantly lack the immune response to a growing tumour [39–41]. This past decade cancer organoids have emerged as a novel three-dimensional system to study both physiological and pathological processes. Organoids are 3D cultured multicellular clusters, that exhibit self-renewal and self-organizing properties [42]. They can be generated either by embryonic (ESC), adult (ASC), induced (iPSC) or cancer (CSC) stem cells [43]. In a pioneer study in 2009, Sato et al. established for the first time 3D epithelial organoids from leucine-rich repeat-containing G-protein coupled receptor 5 (LGR5) $^{+}$ intestinal cells embedded into Matrigel and cultured in medium [44]. Lgr5 is a transmembrane-G-protein coupled receptor, which, after the binding of its ligand R-spondin, activates the Wnt/β-catenin pathway and is used as a marker for stem cells in the intestine. These organoids maintained the crypt-villus structure of the intestine in vitro without a mesenchymal niche. Ever since various a large number of organoids have been developed from many organs including breast [45], brain [46,47], liver [48], lung [49], pancreas [50], stomach [51], oesophagus [52], endometrium [53] and prostate [54].

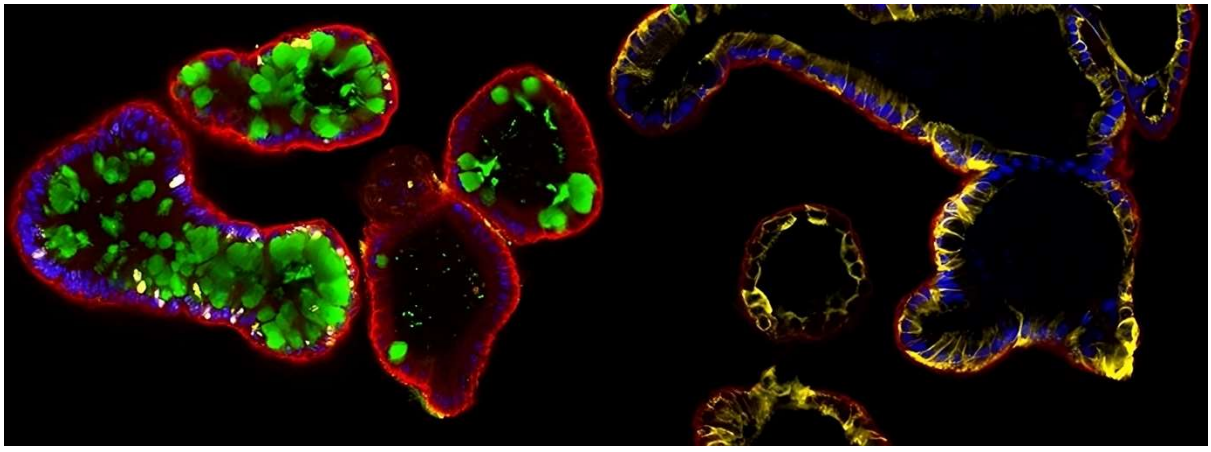

Figure 5: Intestinal organoids under the fluorescent microscope. Source: https://www.stemcell.com/technical-resources/area-of-interest/organoid-research/intestinal-research/mini-review.html

Organoids can be extended long-term, cryopreserved, and genetically modified. They preserve the histopathological features of the original tumours and their heterogeneity and genetically resemble the tumour epithelium they derived from [40]. Therefore, characterizing organoids at the transcriptomic, proteomic and epigenomic levels through both bulk or single-

cell analysis enables a better understanding of the underlying mechanisms of cancer initiation and development [55]. Moreover, this novel 3D system can be used as a simplified and faithful model to study the underlying mechanisms of tumour invasion and metastasis [41]. Patient-derived organoids (PDOs) are organoids, that are directly established from surgical resections, tissue biopsies, circulating tumour cells or ascitic fluid. Currently, many PDOs from diverse types of cancer and matching healthy organoids have been generated and have established living biobanks. This provides a powerful tool for drug development and testing, as PDOs can forecast patient responses in clinical trials, and therefore it can be useful for high throughput anti-cancer screening and personalized medicine programmes [39–43,55,56].

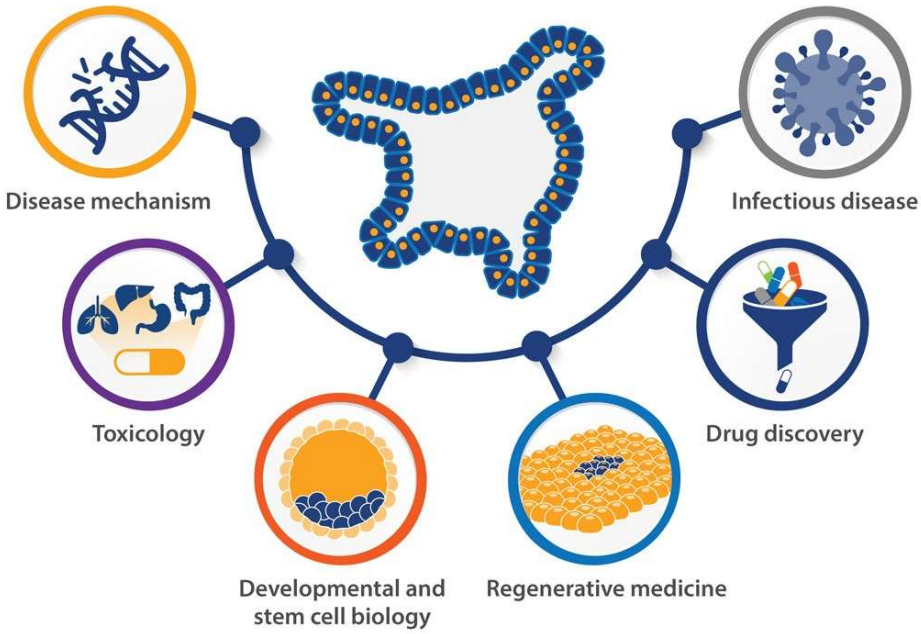

Figure 6: Key applications of organoids. Source: Crown Bioscience

Aim

Metastasis is a multi-step process, that is responsible for more than 90% of cancer-related deaths and due to its complexity, it is significantly difficult to study. Despite the ongoing research and the advancements in the field of clinical oncology, the metastatic process is still poorly understood. Throughout the years, many assays have been implemented using cell lines to gain insight into the invasive potential of cancer cells. However, they do not represent accurately the physiologically relevant environment, as cell lines lack dimensionality. For this reason, it has been deemed crucial the setting up of a 3D assay, that would allow the evaluation of the invasive properties of patient-derived organoids (PDOs), that recapitulate faithfully the tumor of origin. Normal, tumor and metastasis PDOs, that have previously been established in the laboratory, were transduced with lentiviruses expressing the green fluorescent protein (GFP) gene, achieving a stabile expression, and allowing quantitative results. The GFP^+ patient-derived organoids were cultured in two different compositions of matrices: 100% Matrigel (10 mg/dl) and Matrigel (3 mg/dl)-Collagen type I (3 mg/dl) and their morphological changes, that were observed with time-lapse imaging, were then correlated with the expression of genes known to be involved in the process of metastasis.

2. Materials and methods

2.1 Establishment of organoids

Normal, tumor and metastatic organoids were established in the laboratory from surgical resections received from Fondazione IRCCS Istituto Nazionale dei Tumori, Milan, Istituto Neurologico 'Carlo Besta', Milan and Ospedale Niguarda Ca' Granda, Milan. Written informed consent was obtained from all patients for the usage of their samples for research purposes, including the creation of PDOs.

After removal of the transfer medium, each different tissue was minced and transferred into a gentleMACS C tube, in which the three enzymes (enzyme A, enzyme H, enzyme R) from the MACS® Tissue Dissociation Kit (Miltenyi Biotech) and Rock inhibitor were added. The C tube was placed into the gentleMACS™ Dissociator (Miltenyi Biotech) and the proper program according to the type of tissue was chosen. The single-cell suspension was then filtered, in order to remove fibre and the undigested pieces, and centrifuged. Finally, the pellet was washed and plated with Matrigel® Growth Factor Reduced Basement Membrane Matrix, Phenol Red-Free (Corning). Matrigel is a commercialized basement membrane material, that is extracted from Englebreth-Holm-Swarm mice tumors. It mainly contains the ECM proteins laminin, collagen IV, entactin and several growth factors.

2.2 Culture of organoids

The organoids were cultured in a proper medium, which contained all the factors, that have been previously described in studies as necessary for the organoids' expansion and long-term maintenance [43].

Basal culture medium

Components	Final concentration
Advanced DMEM F-12 (Life Technologies)	100%

Penicillin-streptomycin (Euroclone)	1X
Gentamycin (Sigma-Aldrich)	1X
HEPES (Life Technologies)	1X
GlutaMAX (Life Technologies)	1X
B27 supplement (Life Technologies)	1X
N-2 supplement (Life Technologies)	1X
Nicotinamide (NAD) (Sigma-Aldrich)	10 mM
N-acetylcysteine (NAC) (Sigma-Aldrich)	1 mM

Table 1: Composition of basal culture medium

Starting from basal medium, ENAS and WENRAS medium are obtained for the culture of the colorectal and normal PDOs respectively. Wnt3A-conditioned medium is not added in the CRC's medium, as in colorectal cancer the Wnt/β-catenin pathway is constitutively activated due to the mutational background, while in the normal organoids is used to maintain stemness [43]. Metastatic organoids are cultured in ENAS medium as well. Noggin, which is a Bone Morphogenetic Protein inhibitor (BMP) is also added to the medium for stem cell niche maintenance. ROCK inhibitor (Y-27632) is used to prevent anoikis, a type of cell death that occurs in anchorage-dependent cells in case of detachment from the surrounding extracellular matrix [43]. A83-01 and SB202190 act as TGF-β and p38 MAPK inhibitors respectively and have been shown to increase the efficiency of organoids' derivation and maintenance [43].

Component	Final concentration		Dilution
	WENRAS medium	ENAS medium	
Basal medium	50%	100%	
Wnt3A-conditioned medium	50%	-	
EGF (Peprotech)	50 ng/ml	50 ng/ml	1:5000
Noggin (Peprotech)	100 ng/ml	100 ng/ml	1:5000
R-spondin1 (RSPO1)	1 μg/ml	-	1:1000

A83-01 (Tocris)	500 nM	500 nM	1:5000
SB202190 (Sigma)	10 μM	10 μM	1:3000
Gastrin (Sigma)	10 nM	10 nM	1:50000
ROCK inhibitor (Y-27632)	10 μM	10 μM	1:1500

Table 2: Composition of growth medium for human organoids

The medium was changed with a fresh one every 3 days.

2.3 Passage of organoids

The organoids were monitored every 2-3 days and, if it was deemed necessary after observation under the light microscope, they were split. The two ways of passaging organoids for maintenance are the usage of either TrypLE™ Express (ThermoFisher, 12605010) or Cell Recovery Solution. The method, that was chosen each time, was depended on the growth of the organoids. The TrypLE method was used to dissociate the organoids, while the Cell Recovery Solution was preferred in case of matrix change.

TrypLE™ Express Enzyme protocol

After medium removal, each well was washed with cold Phosphate-buffered saline (PBS) containing penicillin-streptomycin and gentamycin. In order to dissolve the Matrigel, 500 μl of pre-warmed TrypLE™ Express with ROCK inhibitor (to a final concentration of 10 μl) was added into each well, and after rinsing the tip with PBS + 1% FBS, the Matrigel drops were resuspended and each well was transferred into a 15 ml falcon tube. The TrypLE solution was blocked by diluting with cold PBS containing penicillin-streptomycin and gentamycin and the organoids were centrifuged at 800×g for 3 minutes at 4^{o}C. After removing the supernatant, the pellets containing the organoids were resuspended with 1 ml cold PBS + 1% FBS and the content was transferred into microcentrifuge tubes, which were then centrifuged again at

800×g for 3 minutes at 4°C. The supernatant was removed, and the organoid pellets were resuspended in the proper amount of Matrigel depending on the splitting ratio and plated in 24-well plates. Once the Matrigel drops had solidified, pre-warmed WENRAS and ENAS medium containing the ROCK inhibitor Y-27632 was added into the normal and CRC organoids respectively and the plates were incubated at 37°C, 5% CO_2.

Cell Recovery protocol

The organoids medium was discarded and each Matrigel drop was washed with cold PBS containing penicillin-streptomycin and gentamycin. Once the Cell Recovery Solution was added into each well and the tip of the pipette was rinsed with cold PBS + 1% FBS, each drop was scraped of the well and the content was transferred into a falcon tube. After the tubes were kept on ice for 30 minutes, cold PBS containing penicillin-streptomycin and gentamycin was added and the organoids were centrifuged for 3 minutes at 800×g. The pellet of organoids was then resuspended in PBS + 1% FBS, transferred into eppendorf tubes and spun down again at 800×g for 3 minutes. After removal of the supernatant, the proper amount of Matrigel was added and the organoids were seeded in pre-warmed 24-well plates. The plates were incubated to allow the Matrigel drop to polymerize, proper pre-warmed culture medium containing the ROCK inhibitor Y-27632 was then added and the plates were incubated again (37°C, 5% CO_2).

2.4 Culture of HEK-293T cells

Human embryonic kidney 293 (HEK293) cells are an immortalized cell line, which derives from a single healthy, electively terminated female fetus [57]. Here, HEK293T cells were used as packaging cells for the production of lentiviral particles since they are easily transfectable and support the high-level expression of viral proteins.

HEK293T cells grow in adhesion; for splitting, medium was removed, and 5 ml of PBS were carefully added to the culture dishes, which were moved around to wash off the media from the whole surface. PBS was then aspirated, and 1 ml of trypsin was added to each dish.

Incubation at 37°C for 5 minutes was followed and 10 ml of pre-warmed serum-containing complete Dulbecco's Modified Eagle Medium (DMEM) was added to block the activity of trypsin. Cells were centrifuged at room temperature for 5 minutes at 500×g and the pellet was resuspended in warm complete DMEM. The proper number of cells was plated, according to the desired splitting ratio.

2.5 Lentiviral vectors (LVV) production

Lentiviruses are produced using a 2nd-generation lentiviral system, comprised of three plasmids. HEK293T cells were transfected with a single packaging plasmid (psPAX2) encoding the HIV-1 Gag, Pol, Rev and Tat genes and a second separate VSV-G envelope plasmid (pMD2.G). As a transfer, plasmid PRRLSIN.cPPT.PGK-GFP.WPRE was used, which contained the gene encoding for the green fluorescent protein (GFP).

Polyethylenimine (PEI), which was used in Mix B, is a stable cationic polymer, which positively charges and forms a complex with DNA. This DNA-PEI complex is endocytosed by the cells and DNA is released into the cytoplasm [58].

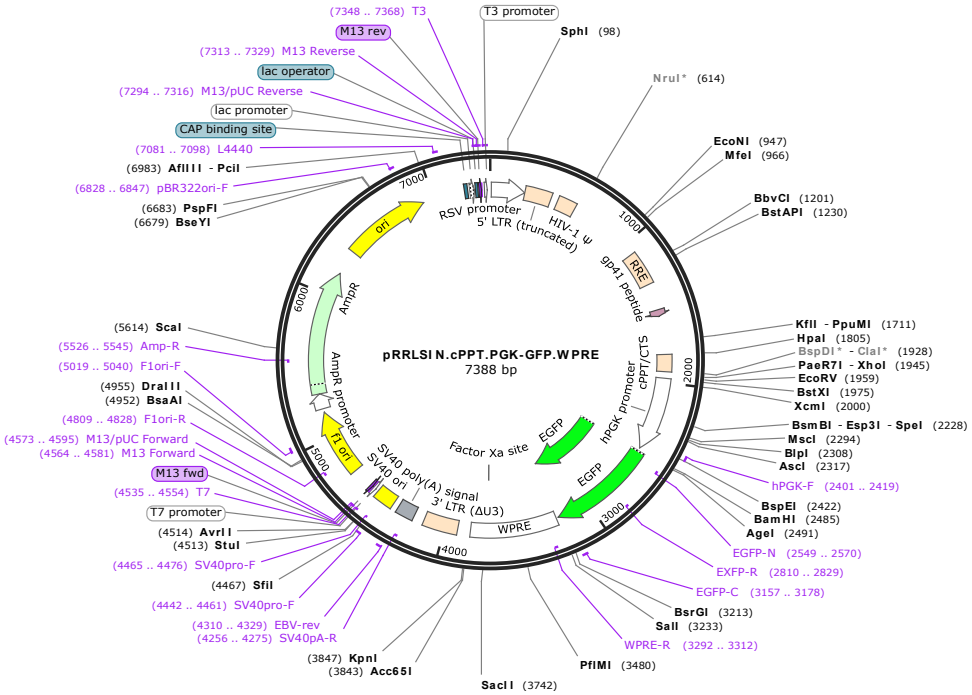

Figure 7: Physical map of transfer plasmid pRRLSIN.cPPT.PGK-GFP.WPRE (addgene)

The day before the transfection, ~ 15M of HEK293T cells were plated in two 15 cm dishes (15M/dish). Starting the procedure, the HEK293T cells were checked under the microscope to ensure that they were in a replication state and their confluency was optimal (around 70%). Firstly, the medium was removed from the culture plate and replaced with 18 ml of pre-warmed Opti-MEM medium. The plates remained in the incubator, while Mix A and B were being prepared according to Table 3 and Table 4. The ratio of PEI to DNA was 3:1.

Mix A	
Components	Amount
pMD2.G (1 μg/ml)	8 μg
psPAX2 (1 μg/ml)	16 μg
transfer vector (1 μg/ml)	25 μg
Opti-MEM	to 500 μl

Table 3: Composition of mix A containing the packaging, envelope and transfer plasmids and culture medium

Mix B	
Components	Volume
PEI (1 μg/ml)	147 μg
Opti-MEM	to 500 μl

Table 2: Composition of mix B containing the polymer and culture medium

Mix B was added to mix A and after vortexing, the solution was incubated for 20 minutes at room temperature. The final mix was released on the surface of the culture dish continuously and it was equally spread by rocking gently the dish, which was afterwards put into the 37 °C incubator in 5% CO_2 overnight or for at least 8 hours. At the end of the incubation, the

transfection medium was replaced with warm complete DMEM. 48 hours post medium change, the supernatant was collected and LVV were pelleted by centrifuging at 2000×g for 2 hours at 4°C. The supernatant was discarded, and the pellet was then resuspended in ~200 µl of complete DMEM. Resuspension was carried out either by pipetting or by using a shaker for 1 hour at 4°C. Concentrated LVVs were aliquoted (10 µl aliquots) and stored at -80°C.

2.6 Titration

The day before the titration, 200k HEK293T cells were plated in a 12-well plate. The next day, two wells were detached and counted (mean = 460k). The culture medium was removed and substituted with 500 µl of DMEM + polybrene (2X). The viral dilutions were the following: 10^{-3}, 10^{-4}, 10^{-5} and 10^{-6}. Finally, 500 µl of each dilution was added to the cells in duplicate and the cells were incubated. After 24 hours, the cells were detached, fixed with 1% paraformaldehyde and through FACS analysis, the percentage of GFP^+ was determined. The 10^{-5} dilution was used to calculate the titer, which resulted 2.5×10^9 TU/ml. The lentiviral titer is measured as Transduction Units per ml (TU/ml).

2.7 Organoids infection

The protocol followed for the lentiviral transduction of the organoids was developed and published in Nature Protocols by Lin Shih-Ching et al. in 2022 [59].

Organoids were dissociated with the TrypLE™ Express (ThermoFisher, 12605010) as previously described and, in order to obtain a single-cell suspension, they were incubated for 5 minutes at 37°C and pipetted about 50 times. The degree of dissociation was checked at the microscope and the incubation/pipetting was repeated if necessary. The content of the wells was transferred into falcon tubes and the TrypLE solution was blocked by diluting it with cold PBS containing antibiotics. After centrifugation at 300×g for 5 minutes at 4°C, the pellet was then resuspended in 500 µl of CMFG (-), composed of Advanced DMEM F-12, 1X penicillin-streptomycin, 10 mM HEPES and 1 mM GlutaMAX. The cells were counted under the light microscope by adding Trypan Blue (diluted 1:2) to evaluate the viability. The total number of

cells was calculated taking into consideration the volume and dilution factor. The desired number of cells to be infected was brought to a final volume of 500 μl and centrifuged at 300×g for 5 minutes at 4°C. The pellet was kept on ice while the concentrated lentiviral solution was prepared as follows:

- 300 μl of CFMG (-)
- 10 μM ROCK inhibitor Y-27632 (1:1500)
- 8 μM of polybrene (1:2600)
- Lentiviral stock to achieve MOI (Multiplicity Of Infection) =5

Polybrene (Hexadimethrine bromide) is a cationic polymer, that is used to increase the efficiency of gene transfer [60]. The pellet was resuspended in the lentiviral solution and transferred to a 48-well plate, which was sealed with parafilm for safety reasons. A negative control, in which no lentiviral particles were added, was always generated. After 5 minutes of incubation at 37°C, the plate was centrifuged at 300×g for 1 hour at room temperature. At the end of the spinoculation, the supernatant was discarded, and the cells were resuspended in 500 μl of ice-cold CMGF (-) and transferred into a new tube in order to be centrifuged at 400×g for 5 minutes. The pellet was resuspended in the proper amount of Matrigel and after the drop had solidified, pre-warmed WENRAS and ENAS culture medium containing the ROCK inhibitor Y-27632 was added into the normal and CRC organoids respectively.

2.8 Fluorescence-activated Cell Sorting (FACS)

The organoid, that were transfected with the lentiviruses, were associated into single cells, stained for Live/Dead APC-Cy7 to determine the viability and sorted at a FACS analysis machine. The GFP positive (GFP^+) normal, tumor and metastatic organoids' population were then plated and maintained in 24-well plates.

2.9 Invasion assay

In order to evaluate the invasive properties of the normal, tumor and metastatic patient-derived organoids, that were previously established, a 3D culture system was set up. The first

experiment was performed utilizing non-GFP$^+$ organoids, in order to test the proper concentrations and the right time points.

The collagen solution (pH=7) was prepared on ice by adding in an eppendorf tube basal medium (1x), 1,2% $NaHCO_3$, HEPES (1M), NaCl (1M) and rat tail Collagen type I in a final concentration of 3 mg/ml.

The organoids were culture in three different conditions: 100% Matrigel (10 mg/dl), 7 mg/dl Matrigel - 1.5 mg/ml rat tail Collagen type I and 3 mg/dl Matrigel - 3 mg/ml rat tail Collagen type I.

The experiment was repeated with the respective GFP$^+$ organoids. 10 µl of Matrigel were used to create a thin coat at the bottom of each well of the µ-Slide 8-well chamber. In parallel, the same organoids were plated 24-well plate for the extraction of RNA. The conditions in the two plates were identical. The Cell Recovery solution protocol was used in each sample to allow the detachment of a few Matrigel drops and the organoids pellet were resuspended in the Matrigel (3 mg/dl)-Collagen type I (3 mg/dl) solution.

2.10 Imaging

Imaging in the first experiment was performed using the brightfield microscope. Regarding the second experiment utilizing GFP$^+$ organoids, Olympus inverted BX81 was used for the brightfield and fluorescent images and Leica TCS SP8-STED for the acquisition of images across the different timepoints (day 1, 3, 5, 8, 10, 12). The analysis of the images was performed in image J and by utilizing bioinformatic tools.

2.11 RNA extraction

The isolation of the RNA was completed using TRIzol following the manufacturer's instructions. TRIzol is a solution that consists of guanidinium isothiocyanate in a single phase

and has the ability to both solubilize biological material and denature proteins simultaneously [61].

The organoid cultures were checked under the microscope to ensure a well-formed morphology and make sure the absence of dead organoids, which equals degraded RNA.
At first, the culture medium was removed and one or two wells were lysated with 1 ml of TRIzol™ Reagent (ThermoFisher) by resuspending up and down until homogeneous and transferred into a 1.5 ml eppendorf. After a 5-minute incubation, 0.2 ml of chloroform was added to the eppendorf, which was then vigorously shaken to achieve a thorough mix. After a 2–3-minute incubation, the samples were centrifuged at 12.000×g for 15 minutes at 4°C. The centrifugation separated the mixture into three different phases: 1. lower organic layer, which contained DNA and proteins, 2. Interphase, which was consisted of a small quantity of DNA and 3. upper aqueous phase, which was comprised of the RNA. Carefully without disrupting the other phases, the upper layer was collected and transferred into a new tube, in which 0.5 ml of isopropanol was added. Following a 10-minute incubation at 4°C, the tube was centrifuged at 12.000×g for 20 minutes at 4°C and the supernatant was removed. The pellet containing the RNA was then resuspended in 1 ml of 70% ethanol, in order to be washed and another centrifuge at 12.000×g for 5 minutes at 4°C followed. Once the supernatant was discarded, the RNA pellet was left to air-dry for a few minutes and then resuspended in 20 μl of RNase-free water. Finally, the tube was incubated in a heat block set at 55-60°C for 15 minutes and treated with DNase to remove any possible DNA contamination. Into the tube containing the RNA, 0.1 volume of 10X TURBO DNase™ Buffer and 1 μl of TURBO DNase™ Enzyme were added, and the tube was incubated for 20-30 minutes at 37°C. DNase Inactivation Reagent (2μl or 0.1 volume, whichever is greater) was added and incubated for 5 minutes at room temperature, flicking the tube 2-3 times, in order to disperse the DNase Inactivation Reagent. After centrifugation at 10.000×g for 1.5 minutes, the supernatant containing the RNA was transferred into a new microcentrifuge tube. RNA quantity and quality were then assessed with Nanodrop and the samples remained in the -80 °C, until usage.

2.12 cDNA synthesis

The kit, that was used for the synthesis of cDNA, was the Invitrogen™ SuperScript™ III First-Strand Synthesis SuperMix for qRT-PCR and it was performed according to the manufacturer's instructions. The kit is composed of:

- RT Enzyme Mix: SuperScript™ III RT and RNaseOUT™, which is an RNase inhibitor protein
- RT reaction mix: oligo$(dT)_{20}$ (2.5 µM), random hexamers (2.5 ng/µl), 10 mM $MgCl_2$, and dNTPs
- E. coli RNase H

For each reaction, a Reverse transcriptase minus (RT -) negative control was used, in which every reagent was added except for the RT enzyme, in order to rule out any possible genomic DNA contamination.

2.13 Real-time quantitative Polymerase Chain Reaction (qPCR)

In order to correlate the invasive phenotype with a 3D matrix-dependent gene expression, qPCR was performed using the TaqMan® Universal PCR Master Mix, No AmpErase® UNG kit with pre-optimized TaqMan® Gene Expression Assay. GAPDH and ACTB were used as housekeeping genes for the normalization of the expression levels. The final mix contained the TaqMan mastermix, TaqMan assay, cDNA and nuclease-free water. Each assay was performed in triplicates for a better statistical outcome.

3. Results

3.1 Phenotype of normal, tumor and metastasis patient-derived organoids

For the first experiment, non-GFP^{+} normal, tumor and metastasis PDOs were cultured under the three different conditions mentioned before (100% Matrigel 10 mg/dl, Matrigel 7 mg/ml-Collagen 1.5 mg/dl, Matrigel 3 mg/dl-Collagen 3 mg/dl). The end-point of the experiment was after 10 days, as the organoids required to be slitted. Images were taken under the brightfield microscope during the timepoints to assess the phenotypic change.

The normal patient-derived organoids cultured in Matrigel after 10 days showed, as expected, a crypt-like budding structure, while the organoids cultured in the increasing concentrations of collagen were observed to acquire a cystic morphology (Figure 8).

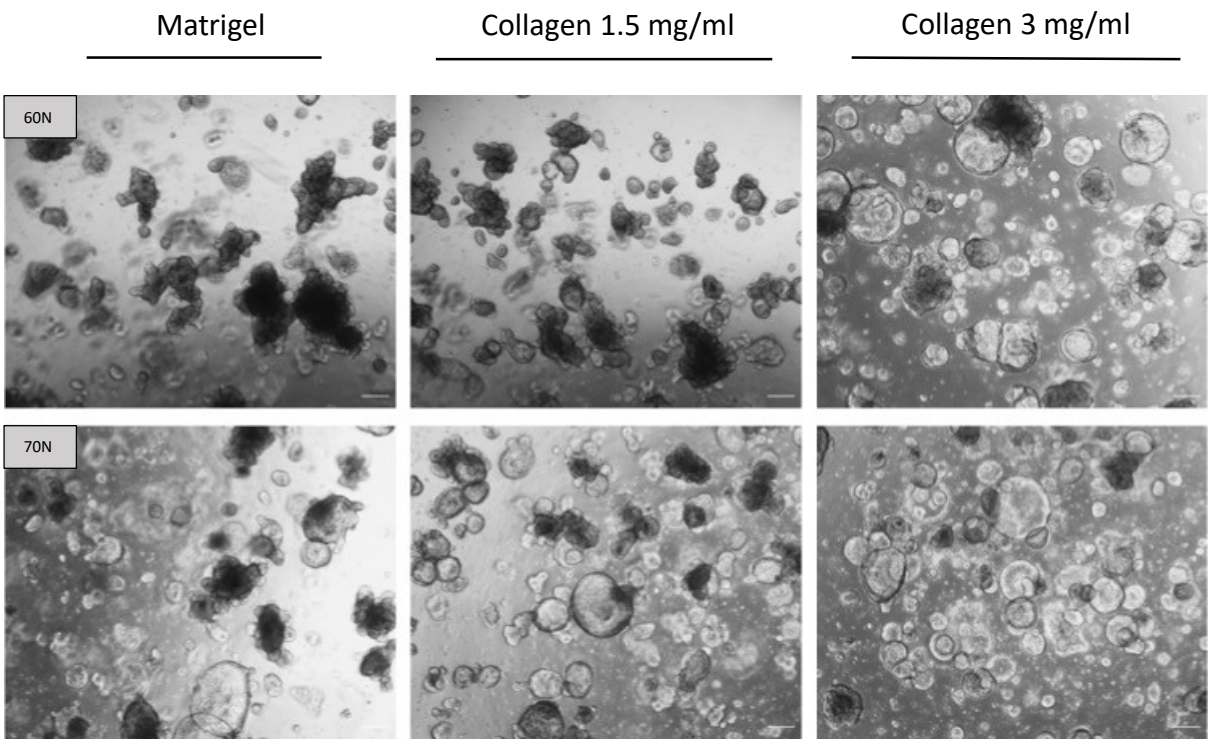

Figure 8: Brightfield images of normal colonic (60N, 70N) patient-derived organoids after 10 days of growth in the three different conditions. Exposure to increasing concentrations of collagen induces a cystic morphology.

Concerning the tumor PDOs, no phenotypic change was observed between the two conditions (Figure 9).

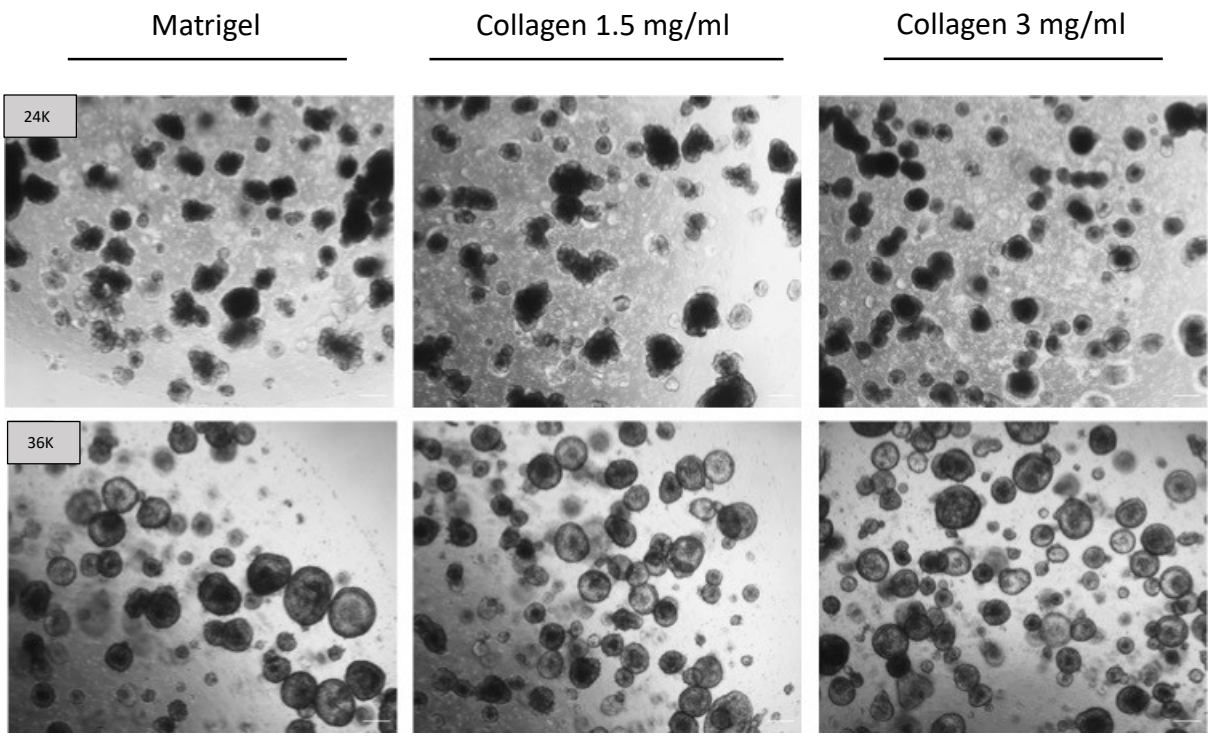

Figure 9: Brightfield images of colorectal cancer (24K, 36K) patient-derived organoids after 10 days of growth in the three different conditions. Exposure to increasing concentrations of collagen did not affect the phenotype. Scale Bar: 100µm

The two metastasis PDOs behaved differently when cultured in collagen type I. CBM1 seemed to acquire an invasive phenotype with distinct protrusions, that could be observed under the microscope. However, no phenotypic changes were observed in CBM3 when cultured in collagen (Figure 10). The protrusions and the spreading phenotype of CBM1 cultured in collagen type I (3 mg/ml) can be appreciated better with higher magnification (Figure 11).

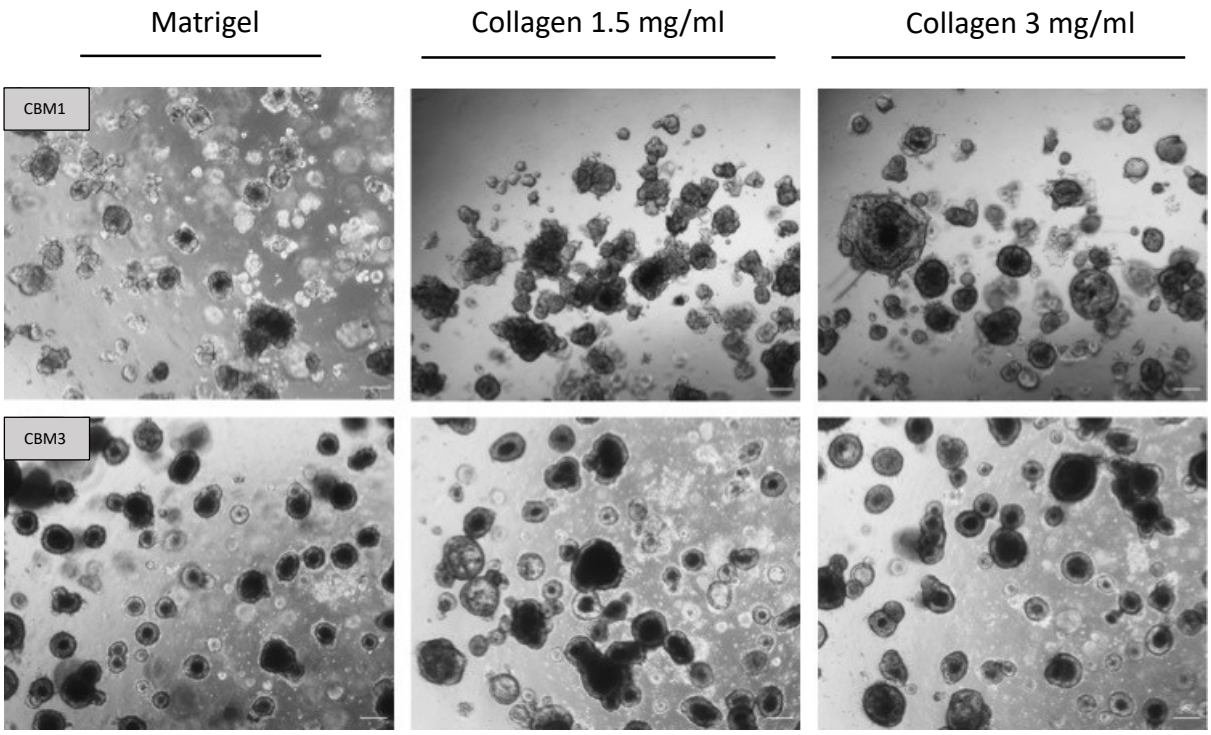

Figure 10: Brightfield images of colon-to-brain metastasis (CBM1, CBM3) patient-derived organoids after 10 days of growth in the three different conditions. Exposure to increasing concentrations of collagen induced an invasive phenotype in CBM1, but not in CBM3. Scale Bar: 100µm

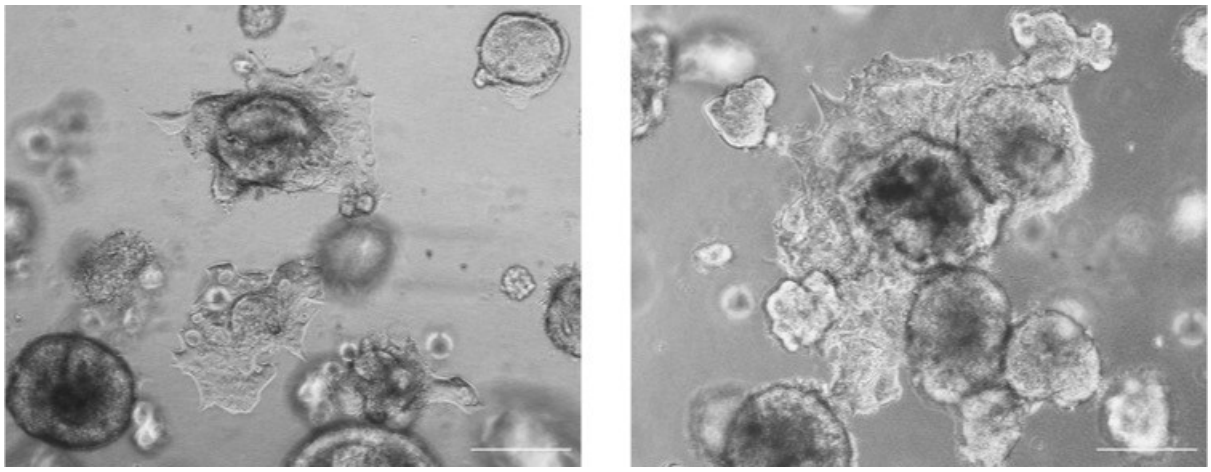

Figure 11: Brightfield images of colon-to-brain metastasis patient-derived organoids (PDOs) CBM1 cultured in collagen type I (3 mg/ml). An invasive phenotype can be appreciated and distinct protrusions are observed. Scale Bar: 100µm

The assay was repeated (experiment 2) utilizing GFP^+ organoids for a more informative quantitative readout. Images taken under the fluorescence microscope validated the observations from the first experiment. Most importantly, CBM1 when cultured in collagen (3 mg/ml) acquired the expected invasive phenotype with distinct protrusions (Figure 12).

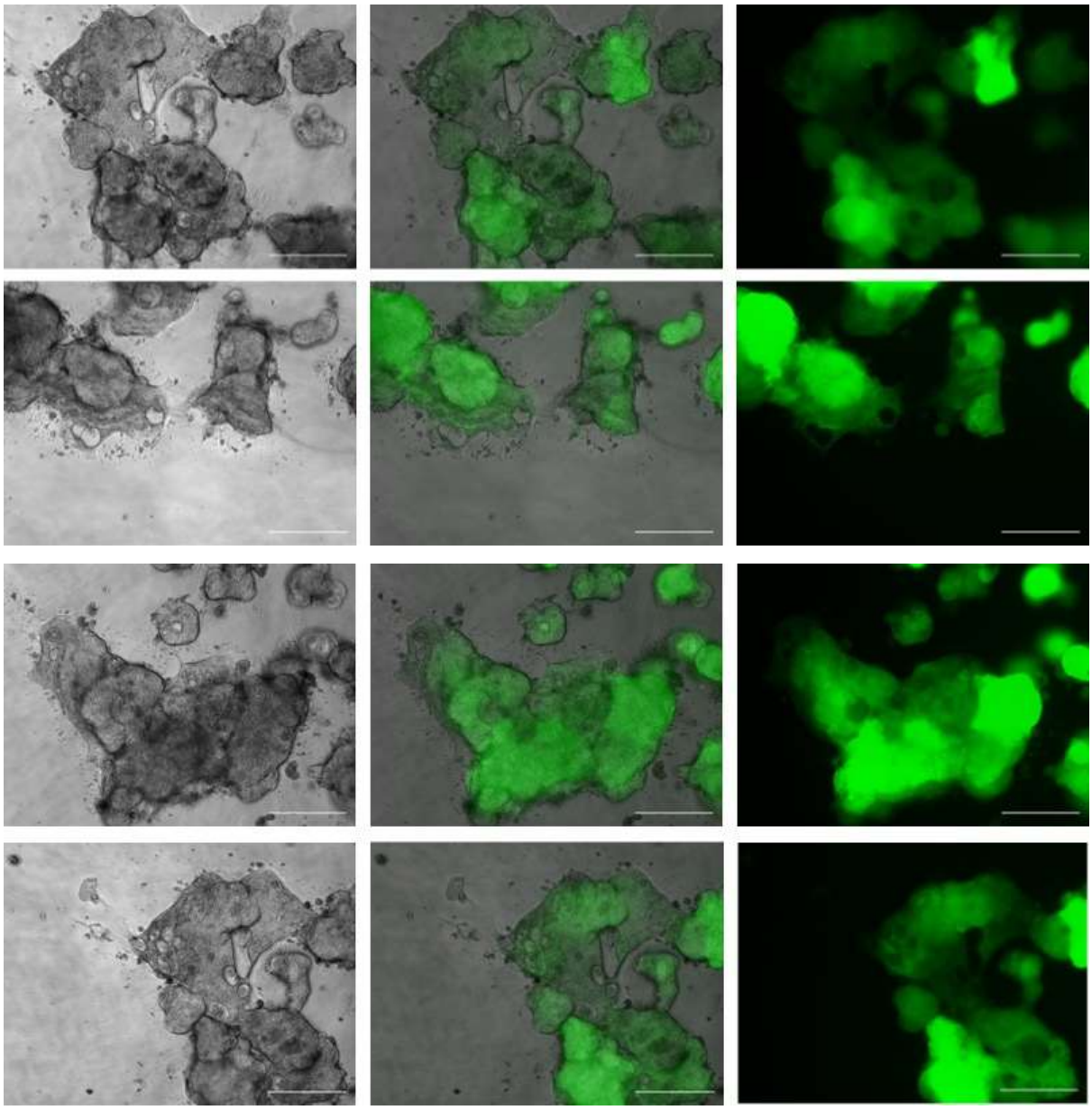

Figure 12: Brightfield and fluorescent images of CBM1 cultured in collagen type I (3 mg/ml). Distinct protrusions can be observed. Scale Bar: 100µm

To gain deeper insights into the influence of extracellular matrix (ECM) composition on the cell behaviour and phenotype, quantitative real-time RT-PCR was employed in both of the two experiments to evaluate the 3D matrix-dependent expression of genes involved in the process of Epithelial-Mesenchymal Transition (EMT). By analysing the gene expression data, it is possible to potentially elucidate the underlying reasons for the divergent phenotypes observed between samples.

3.2 Expression of key epithelial genes

Experiment 1

Between the two metastasis PDOs a significant difference in the expression of epithelial markers was observed. At basal levels, the PDOs differentially expressed the epithelial markers E-cadherin and Epithelial Cell Adhesion Molecule (EpCAM), with CBM1 having higher gene expression levels. Exposure to higher concentrations of collagen type I did not affect the expression levels (graph 1).

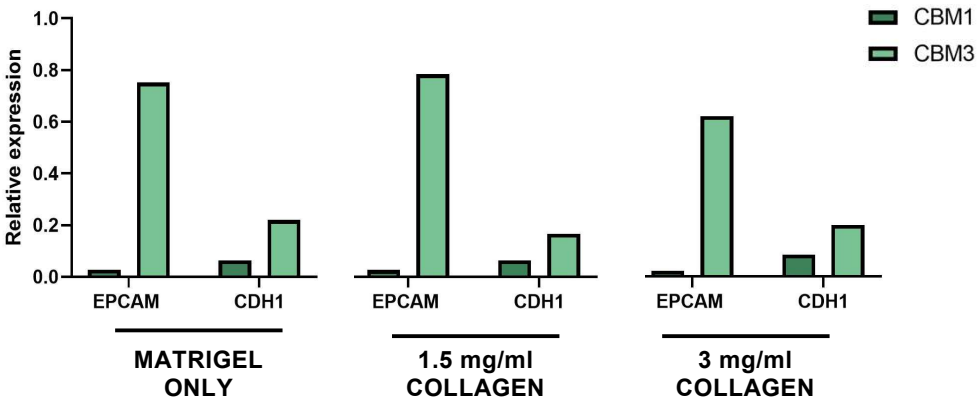

Graph 1: Expression levels of epithelial markers EPCAM and E-cadherin in CBM1 cultured in three different conditions

Regarding the normal PDOs, a lower expression of the markers were observed as the concentration of collagen was increasing (graph 2).

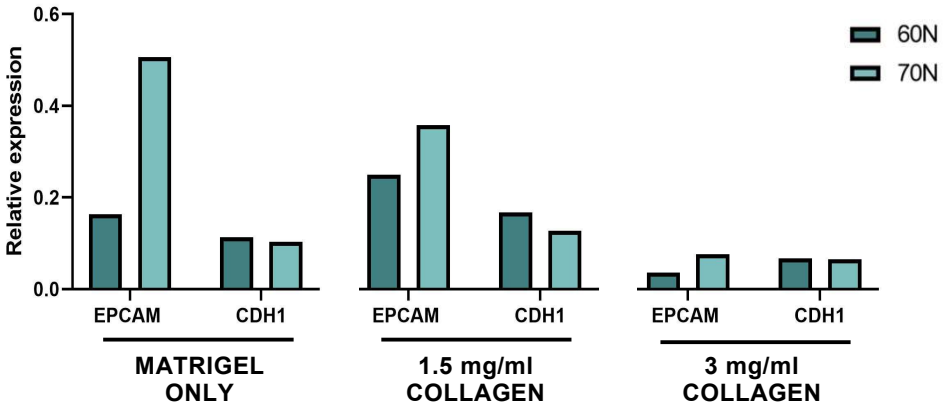

Graph 2: Expression levels of epithelial markers EPCAM and E-cadherin in normal PDOS cultured in three different conditions

Contrary to the other PDOs, in the tumour PDOs, no difference in the expression levels was observed (graph 3).

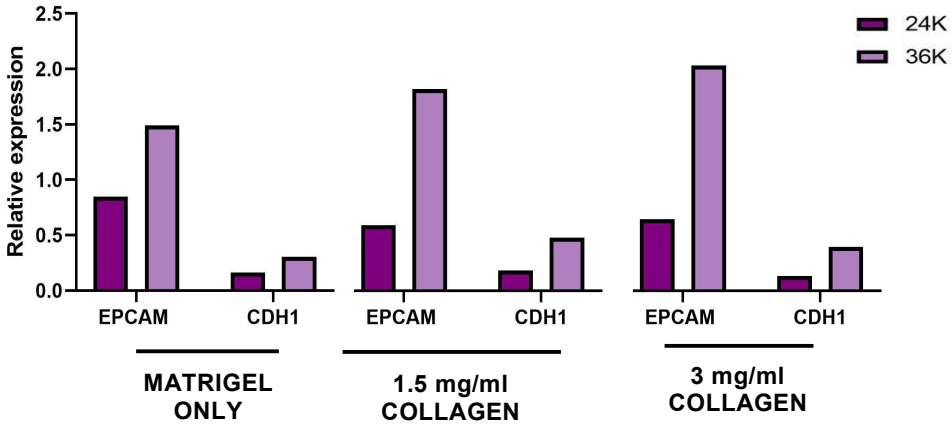

Graph 3: Expression levels of epithelial markers EPCAM and E-cadherin in tumour PDOs cultured in three different conditions

Experiment 2

The gene expression levels observed in the second experiment were in line with the ones from the first experiment

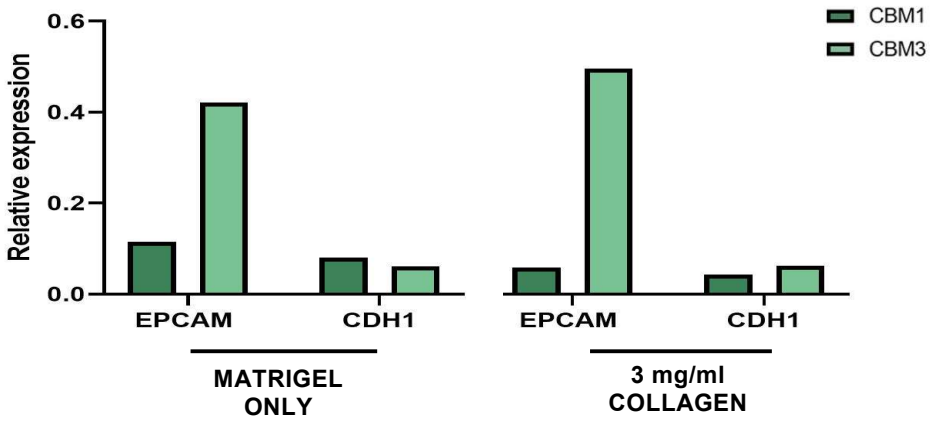

Graph 4: Expression levels of epithelial markers EPCAM and E-cadherin in metastasis PDOs cultured in three different conditions

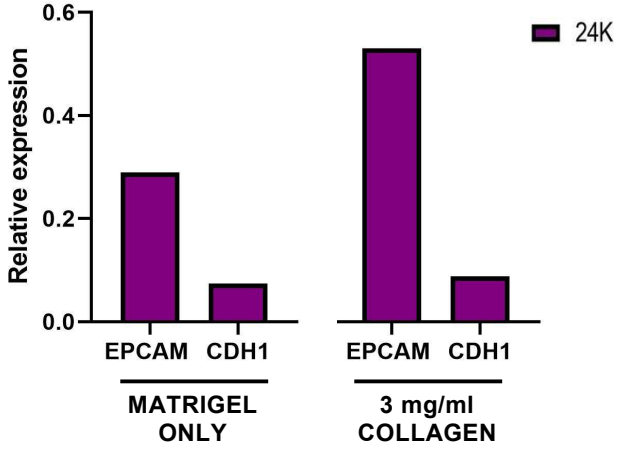

Graph 5: Expression levels of epithelial markers EPCAM and E-cadherin in tumour PDOs cultured in three different conditions

3.3 Expression of key genes EMP1 and L1CAM

Experiment 1

The two metastasis PDOs expressed different levels of EMP1 and L1CAM, with CBM3 unexpectedly expressing higher levels (graph 7).

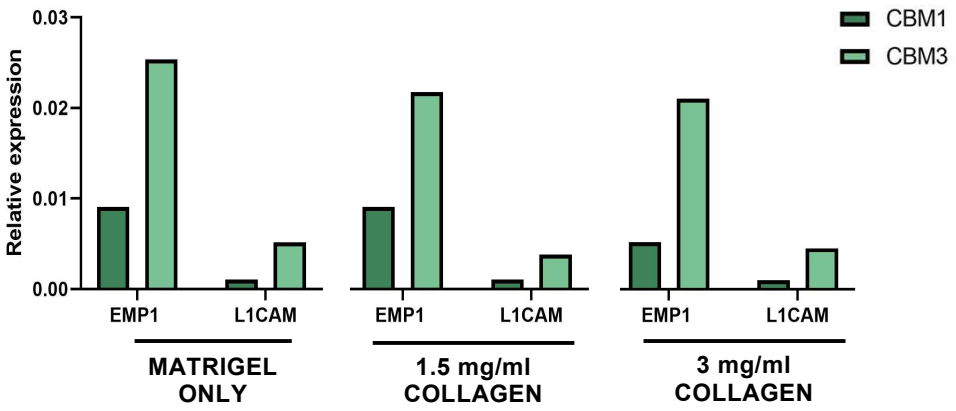

Graph 6: Expression levels of EPCAM and L1CAM in metastasis PDOs cultured in three different conditions

Regarding the tumour PDOs, no alteration was observed in the gene expression levels of the two markers between the conditions (graph 7).

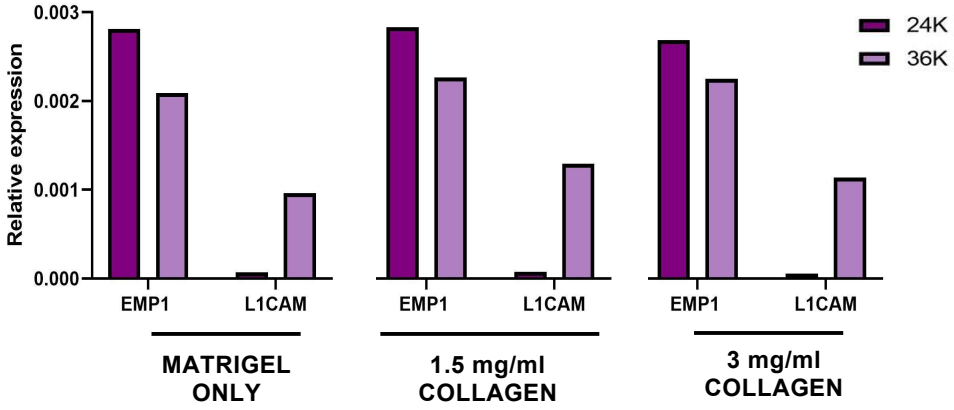

Graph 7: Expression levels of EPCAM and L1CAM in tumour PDOs cultured in three different conditions

Experiment 2

The gene expression levels observed in the second experiment were in line with the ones from the first experiment concerning the tumour PDOs (graph 8).

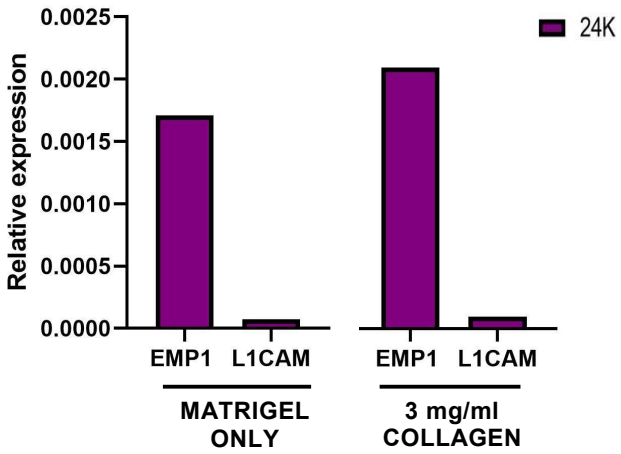

Graph 8: Expression levels of EMP1 and L1CAM in tumour PDO (24K) cultured in Matrigel and collagen (3 mg/ml)

However, concerning the metastasis PDOs, an opposite trend was observed in the expression levels, with CBM1 expressing higher levels of EMP1 and L1CAM (graph 9).

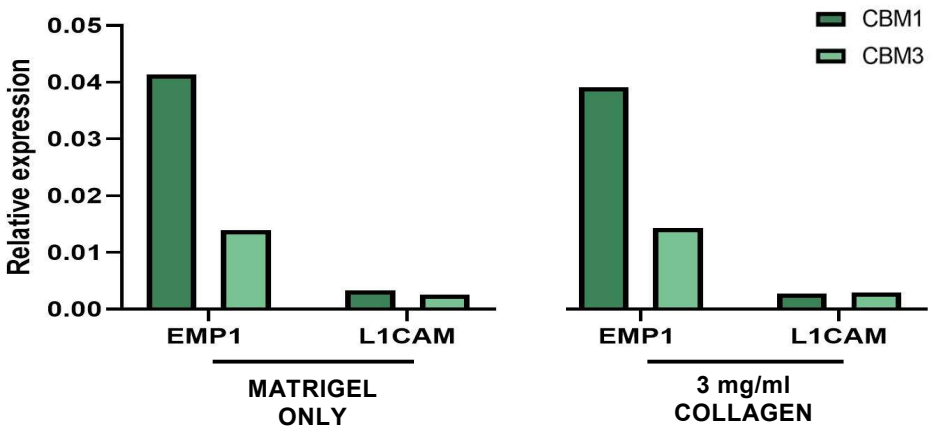

Graph 9: Expression levels of EMP1 and L1CAM in metastasis PDOs cultured in Matrigel and collagen (3 mg/ml)

3.4 Expression of matrix metalloproteinases (MMPs)

Experiment 1

Different expression levels of Matrix metalloproteinases were observed between the two metastasis PDOs. Specifically, CBM1 expressed relatively high levels of MMP1 and MMP2, while no expression was noted in CBM1 (graph 10).

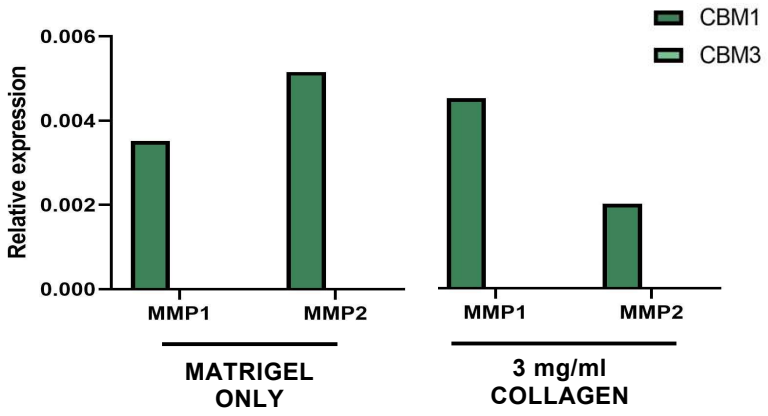

Graph 10: Expression levels of Matrix Metalloproteinases (MMP) 1 and 2 in metastasis PDOs cultured in Matrigel and collagen (3 mg/ml)

Experiment 2

The results of the gene expression levels validated the observations of the first experiment (graph 11).

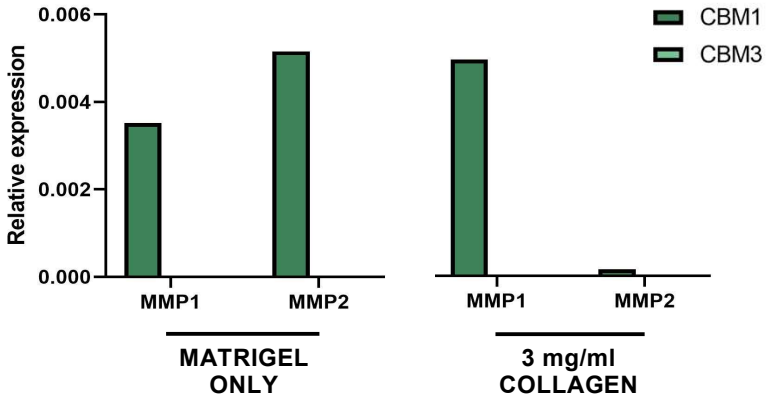

Graph 11: Expression levels of Matrix Metalloproteinases (MMP) 1 and 2 in metastasis PDOs cultured in Matrigel and collagen (3 mg/ml)

3.5 Expression of other genes

The expression levels of other genes (Fibronectin, vimentin, MMP3, MMP7, MMP9, MMP14) were evaluated too. However, no conclusions could be drawn due to the low levels of expression.

3.6 Image segmentation and 3D reconstruction

Images of the organoids across the different timepoints were acquired in order to move towards more complex modelling. To obtain more quantitative information, optimizing the pipeline steps and testing different parameters for smoothing and segmentation is crucial.

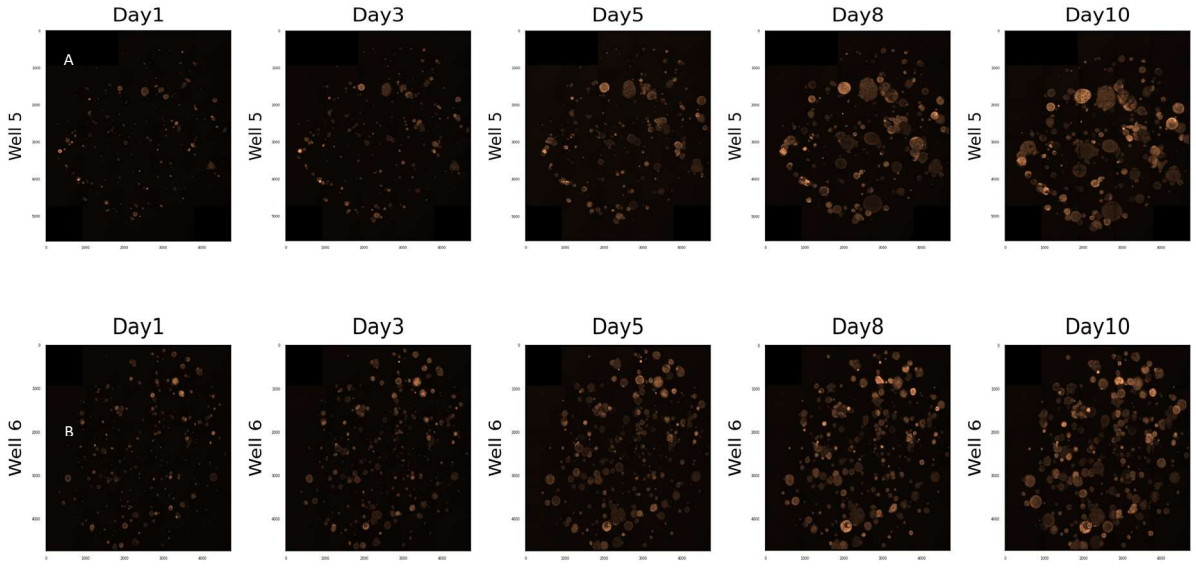

Figure 13: Representative maximal projection images of CBM3 cultured in A) Matrigel and B) collagen (3 mg/ml) across the different timepoints.

3D reconstruction will allow tracking single organoids along time and having a more quantitative analysis of their features (e.g., dimension, volume, circularity, presence of protrusions).

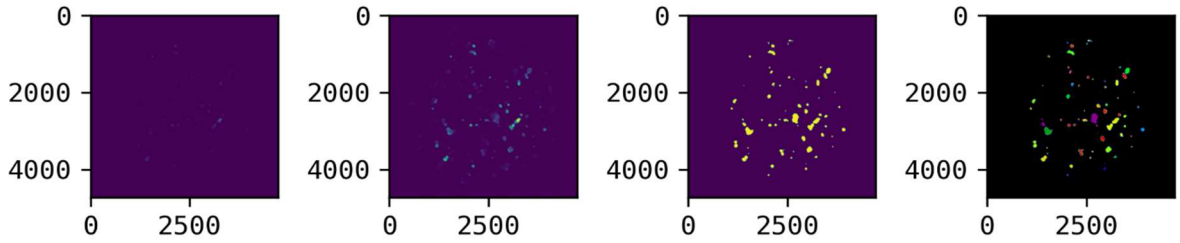

Figure 14: Image segmentation of images acquired from a specific well. Each colour represents a single organoid.

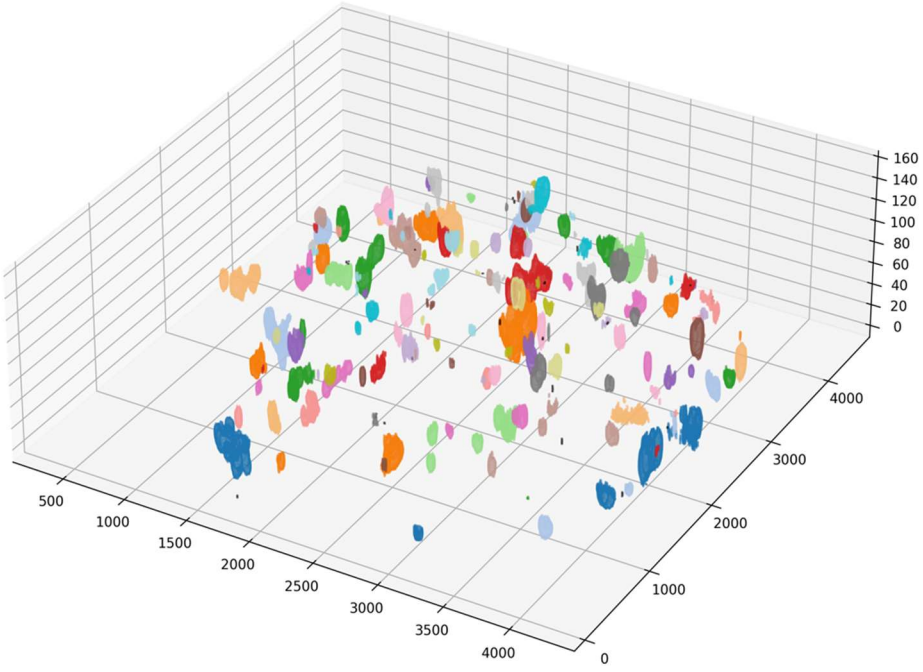

Figure 15: 3D well reconstruction to gain quantitative insights of each single organoid.

Discussion

Metastasis is a complex multi-step process, that is responsible for cancer therapy failure, disease recurrence and is the primary cause of cancer-related deaths. Despite the recent advances in cancer research, metastasis is poorly understood, while treatment remains a challenge. Contrary to primary tumors, which can effectively be treated by local surgery of radiation, metastasis represents a systemic disease [62]. Therefore, fundamental understanding of cancer metastasis is critical in order to develop effective treatments and have improved patient outcome. It is well known that the extracellular matrix modulates the tumor growth and the metastatic journey. One of the defined hallmarks of metastasis, firstly described by Hanahan and Weinberg, is the acquisition of invasive properties, in order to achieve the invasion of local stroma. The development of invasive tumors and their metastatic dissemination involve a series of biologically discrete steps, which are highly associated with distinct alterations in composition, posttranslational modifications, organization and biomechanical properties of the ECM [63]. Matrix metalloproteinases (MMPs) play a critical role in the remodeling of the extracellular matrix and therefore in cancer progression and metastatic cascade. It has been previously reported that the expression of both MMP1 and MMP2 play a critical role in colorectal cancer and at the initial stages of tumor invasion and metastasis [64,65].

Multiple in vitro assays have been implemented in the past to study the migration and invasiveness of cancer cells, such as the wound healing assay and transwell invasion assay. However, these models have limitations and specifically most importantly, they lack dimensionality and therefore cannot be physiologically relevant. These past years advances in 3D cell culturing techniques using organoids and spheroids have allowed the implementation of 3D in vitro assays, which yield much more valuable insights into the underlying mechanisms of metastasis.

In this study, a novel 3D invasion assay was implemented, which allowed the investigation and characterization of the invasive properties of different patient-derived organoids. Specifically, organoids deriving from normal colon tissue, colorectal cancer and colon-to-brain metastasis

were cultured in the two different matrices of Matrigel and Collagen type I. Throughout the days, images were taken under the brightfield microscope, and the phenotypic changes were extensively observed. After reaching the 10-day endpoint, the RNA was extracted to assess and correlate the morphology with the gene expression levels. The same organoid lines were then transduced with lentiviruses achieving a steadily expression of the green fluorescent protein and allowing the better visualization and quantitative outcomes. Utilizing the GFP^+ organoids, the invasion assay was implemented again. To exclude the possibility of organoids spreading in the well, a thin layer of Matrigel was coated in each well. Imaging using the confocal microscope allowed the acquirement of images across different timepoints and are currently used for the 3D reconstruction of the organoids.

Firstly, regarding the phenotypic changes, we observed normal patient-derived organoids acquiring a circular morphology, when exposed to the stiffer ECM of Matrigel-collagen type I. This finding aligns with previous studies reported in the literature. The intestinal epithelium has the ability to renew itself withing 4-7 days, making it the fastest renewing tissue. Intestinal injury can occur due to dietary or chemical compounds, microbes or therapeutical treatment and it is responsible for reactivation of a fetal-like transcriptional program [66]. In a recent study, the phenotypic change from crypt-like to cystic organoid structures was associated with activation of YAP/TAZ pathway to induce a fetal-like regenerative reprogramming of intestinal epithelial cells in an ECM-dependent regulatory manner [67].

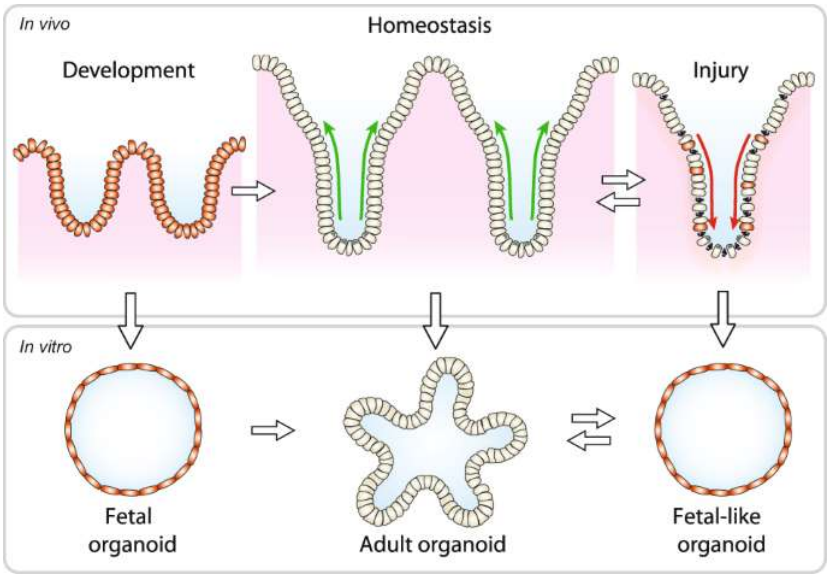

Figure 16: Injury induces a fetal-like regenerative reprogramming through the activation of YAP-TAZ pathway. Source: Sprangers, J., et al. Cell Death & Differentiation, 28(1), 95–107.

In another paper it was also shown that stiff non-degradable matrix like collagen type I can induce the same cystic phenotype through YAP-mediated mechanosensing and transduction [68].

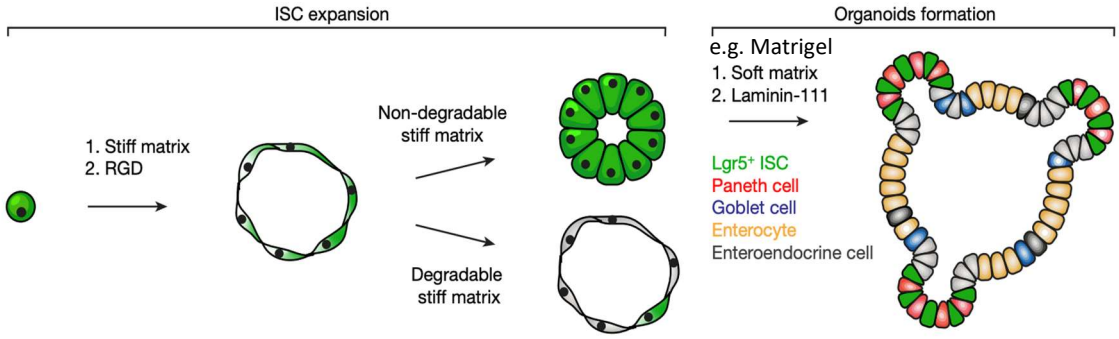

Figure 17: Stiff-degradable matrix e.g., collagen type I induces a cystic phenotype through YAP-mediated mechanosensing and transduction. Source: Gjorevski, N., et al., Nature, 539(7630), 560–564.

This morphology was in line with the gene expression levels, as the epithelial markers EPCAM and E-cadherin were downregulated when the PDOs where cultured in increasing concentration of collagen.

Higher density and altered architecture of fibrillar collagen has been observed in many types of cancer. It has been previously reported that ECM stiffness plays a crucial role as well in cancer metastasis, as tumour cells are able to migrate faster in stiffer ECM. This favours the formation of filopodia, lamellipodia and invadosomes through integrin clustering, focal adhesion kinase (FAK) phosphorylation and Rho GTPase activation and can induce a mesenchymal invasive phenotype[63]. In addition to the to changes in density, the altered composition can also be of huge importance. Matrigel is mainly composed of laminins and collagen IV and is used as a surrogate basement membrane, while the fibrillar collagen type I

is found in connective tissue and predominantly in the intestinal membrane [68]. Remarkably, a changed composition with a shift to collagen type I or type II has been correlated with invasiveness, angiogenesis and reduced survival in invasive ductal carcinomas and melanomas[69]. This observation from the literature is consistent with our findings.

Regarding the metastasis PDOs cultured in the collagen matrix, CBM1 appeared to have a more invasive spreading, phenotype with distinct protrusions and compared to CBM3, in which the morphology did not change. The gene expression levels indicated a lower expression of epithelial markers EPCAM and E-cadherin in CBM1 and a higher expression of MMP1 and MMP2 compared to CBM3. Exposure to increasing concentration of collagen did not affect the expression levels. The two metastasis PDOs have pre-existing differences in the gene expression, which can be due to patients' heterogeneity. Presumably, as collagen acts as a permissive environment, CBM1's invasive potential can be fulfilled when exposed to it. Unexpectedly, in the first experiment the expression levels of EMP1 and L1CAM, were observed higher in CBM3, despite it not acquiring an invasive phenotype, while in the second one, the opposite trend was noted. It is important that the experiment will be repeated again, so the results can be more conclusive. At the same time, even though EMP1 has been associated with metastasis, it is possible that it is part of gene signature with other genes, that were not target in these experiments.

The collagen matrix did not affect neither the morphology nor the gene expression levels of the genes evaluated.

In the future, it is important to extent the experiment and implement the invasion assay to other metastases patient-derived organoids too, in order to shed light into the differences between the invasive potential of not only the same, but also different metastatic sites. This will also allow the detection and assessment of observed patterns, while increasing the reliability of the assay and excluding the influence of extraneous factors.

In this study, we examined the phenotype and gene expression of metastases derived from different patients but originating from the same primary site. Surprisingly, despite the shared primary tumor and metastatic site, crucial differences were observed in both the invasive

phenotype and gene expression profiles. These findings highlight the critical importance of comprehending the molecular basis of such variations in the field of oncology. While metastases may arise from the same primary tumor, the heterogeneity between patients can significantly affect cancer progression and treatment outcomes. Addressing and understanding the underlying mechanisms of the unique characteristics of each patient's metastatic disease can lead to more effective and tailored therapeutic strategies.

The analysis was performed in bulk, while widely used and informative, can have important limitations. Because only a few specific genes were evaluated and their expression was analyzed, it would be of huge importance to perform RNA-sequencing and observe the expression of many other genes. This will also allow the better understanding of the differences between the two metastasis PDOs. Additionally, bulk analysis can result to loss of cellular heterogeneity and masking of subpopulations. Knock-in experiments or implementation of whole-mount staining will be informative to associate the expression of specific genes in distinct subpopulations or with the formation of protrusions.

In this study, patient-derived organoids were used as a model to gain more insights into the invasive potential of cancer cells in 3D. Organoid technology has emerged as a unique tool for modelling and understanding better not only cancer but other human genetic diseases, including Cystic Fibrosis [70], Down Syndrome [71], Parkinson's Disease [72] and Alzheimer's Disease [73] and infectious diseases, like Zika virus [74] and SARS-CoV-2 [75].

However, organoids display disadvantages as well. Generally, they require expertise, are time-consuming and more expensive than 2D cultures, while fresh tumor tissue might not be always available [76]. One of the main intrinsic limitations of organoid culture is the lack of the multicellular nature of tumor microenvironment (TME). TME is comprised of the immune cells including T and B cells, NK cells, tumor-associated macrophages (TAMs), myeloid-derived suppressor cells, dendritic cells, and neutrophils, along with stromal cells, which include cancer-associated fibroblasts, pericytes and endothelial cells and components of ECM [31]. ASC-derived organoids are comprised of only the epithelial compartments, while the tumor stromal fibroblasts, immune cells, vascular endothelial cells, nerves, and microbial factors are absent [39]. In order to overcome this, co-culture systems of PDOs with a variety of cell types

have been developed, which allow the study of the complex crosstalk between the TME compartments. Another robust methodology has been recently described, in which minced tissue deriving from surgical resections is embedded in a 3D matrix scaffold composed of collagen type I under an air-liquid interface (ALI). This not only allows the long-term culture of the PDOs due to improved oxygenation, but also the preservation of complex TME, including immune cells [77].

References

1. Sung H, Ferlay J, Siegel RL, et al. Global Cancer Statistics 2020: GLOBOCAN Estimates of Incidence and Mortality Worldwide for 36 Cancers in 185 Countries. *CA Cancer J Clin*. 2021;71(3):209-249. doi:10.3322/caac.21660
2. Key Statistics for Colorectal Cancer. Accessed March 17, 2023. https://www.cancer.org/cancer/colon-rectal-cancer/about/key-statistics.html
3. Cancer Stat Facts: Colorectal Cancer. Accessed March 17, 2023. https://seer.cancer.gov/statfacts/html/colorect.html
4. Karahalios A, Simpson JA, Baglietto L, et al. Change in weight and waist circumference and risk of colorectal cancer: results from the Melbourne Collaborative Cohort Study. *BMC Cancer*. 2016;16(1):157. doi:10.1186/s12885-016-2144-1
5. Lewandowska A, Rudzki G, Lewandowski T, Stryjkowska-Góra A, Rudzki S. Risk Factors for the Diagnosis of Colorectal Cancer. *Cancer Control*. 2022;29:107327482110566. doi:10.1177/10732748211056692
6. Jarosz M, Sekuła W, Rychlik E. Trends in Dietary Patterns, Alcohol Intake, Tobacco Smoking, and Colorectal Cancer in Polish Population in 1960–2008. *Biomed Res Int*. 2013;2013:1-10. doi:10.1155/2013/183204
7. Baidoun F, Elshiwy K, Elkeraie Y, et al. Colorectal Cancer Epidemiology: Recent Trends and Impact on Outcomes. *Curr Drug Targets*. 2021;22(9):998-1009. doi:10.2174/1389450121999201117115717
8. Rawla P, Sunkara T, Barsouk A. Epidemiology of colorectal cancer: incidence, mortality, survival, and risk factors. *Gastroenterology Review*. 2019;14(2):89-103. doi:10.5114/pg.2018.81072
9. Song M, Garrett WS, Chan AT. Nutrients, Foods, and Colorectal Cancer Prevention. *Gastroenterology*. 2015;148(6):1244-1260.e16. doi:10.1053/j.gastro.2014.12.035
10. Fuchs CS, Giovannucci EL, Colditz GA, et al. Dietary Fiber and the Risk of Colorectal Cancer and Adenoma in Women. *New England Journal of Medicine*. 1999;340(3):169-176. doi:10.1056/NEJM199901213400301

11. Terry P, Giovannucci E, Michels KB, et al. Fruit, Vegetables, Dietary Fiber, and Risk of Colorectal Cancer. *JNCI Journal of the National Cancer Institute*. 2001;93(7):525-533. doi:10.1093/jnci/93.7.525
12. Pietinen P, Malila N, Virtanen M, et al. Diet and risk of colorectal cancer in a cohort of Finnish men . *Cancer Causes and Control*. 1999;10(5):387-396. doi:10.1023/A:1008962219408
13. Tsoi KKF, Pau CYY, Wu WKK, Chan FKL, Griffiths S, Sung JJY. Cigarette Smoking and the Risk of Colorectal Cancer: A Meta-analysis of Prospective Cohort Studies. *Clinical Gastroenterology and Hepatology*. 2009;7(6):682-688.e5. doi:10.1016/j.cgh.2009.02.016
14. Bai X, Wei H, Liu W, et al. Cigarette smoke promotes colorectal cancer through modulation of gut microbiota and related metabolites. *Gut*. 2022;71(12):2439-2450. doi:10.1136/gutjnl-2021-325021
15. Fedirko V, Tramacere I, Bagnardi V, et al. Alcohol drinking and colorectal cancer risk: an overall and dose–response meta-analysis of published studies. *Annals of Oncology*. 2011;22(9):1958-1972. doi:10.1093/annonc/mdq653
16. Boffetta P, Hashibe M. Alcohol and cancer. *Lancet Oncol*. 2006;7(2):149-156. doi:10.1016/S1470-2045(06)70577-0
17. Murata M, Tagawa M, Watanabe S, Kimura H, Takeshita T, Morimoto K. Genotype Difference of Aldehyde Dehydrogenase 2 Gene in Alcohol Drinkers Influences the Incidence of Japanese Colorectal Cancer Patients. *Japanese Journal of Cancer Research*. 1999;90(7):711-719. doi:10.1111/j.1349-7006.1999.tb00805.x
18. Society AC. About Colorectal Cancer: What Is Colorectal Cancer? https://www.cancer.org/cancer/colon-rectal-cancer/about/what-is-colorectal-cancer.html
19. Rawla P, Sunkara T, Barsouk A. Epidemiology of colorectal cancer: incidence, mortality, survival, and risk factors. *Gastroenterology Review*. 2019;14(2):89-103. doi:10.5114/pg.2018.81072
20. Castro ÁG, Iglesias HL. Histopathological diagnosis of CRC. In: *Foundations of Colorectal Cancer*. Elsevier; 2022:149-156. doi:10.1016/B978-0-323-90055-3.00050-8

21. Worthley DL, Whitehall VL, Spring KJ, Leggett BA. Colorectal carcinogenesis: Road maps to cancer. *World J Gastroenterol*. 2007;13(28):3784-3791. doi:10.3748/wjg.v13.i28.3784
22. Saridaki Z, Souglakos J. Genetic alterations in colorectal cancer in older patients. *Management of Colorectal Cancers in Older People*. 2013;(February):9-20. doi:10.1007/978-0-85729-984-0_2
23. Molinari C, Marisi G, Passardi A, Matteucci L, De Maio G, Ulivi P. Heterogeneity in Colorectal Cancer: A Challenge for Personalized Medicine? *Int J Mol Sci*. 2018;19(12):3733. doi:10.3390/ijms19123733
24. Singh MP, Rai S, Pandey A, Singh NK, Srivastava S. Molecular subtypes of colorectal cancer: An emerging therapeutic opportunity for personalized medicine. *Genes Dis*. 2021;8(2):133-145. doi:10.1016/j.gendis.2019.10.013
25. Guinney J, Dienstmann R, Wang X, et al. The consensus molecular subtypes of colorectal cancer. *Nat Med*. 2015;21(11):1350-1356. doi:10.1038/nm.3967
26. Fessler E, Medema JP. Colorectal Cancer Subtypes: Developmental Origin and Microenvironmental Regulation. *Trends Cancer*. 2016;2(9):505-518. doi:10.1016/j.trecan.2016.07.008
27. Welch DR, Hurst DR. Defining the Hallmarks of Metastasis. *Cancer Res*. 2019;79(12):3011-3027. doi:10.1158/0008-5472.CAN-19-0458
28. Fares J, Fares MY, Khachfe HH, Salhab HA, Fares Y. Molecular principles of metastasis: a hallmark of cancer revisited. *Signal Transduct Target Ther*. 2020;5(1). doi:10.1038/s41392-020-0134-x
29. Daniele V, Simeone P, Frank J, et al. Translating epithelial mesenchymal transition markers into the clinic: Novel insights from proteomics. *EuPA Open Proteom*. 2016;10:31-41. doi:10.1016/j.euprot.2016.01.003
30. Williams ED, Gao D, Redfern A, Thompson EW. Controversies around epithelial–mesenchymal plasticity in cancer metastasis. *Nat Rev Cancer*. 2019;19(12):716-732. doi:10.1038/s41568-019-0213-x
31. Gerstberger S, Jiang Q, Ganesh K. Metastasis. *Cell*. 2023;186(8):1564-1579. doi:10.1016/j.cell.2023.03.003
32. Steeg PS. Tumor metastasis: Mechanistic insights and clinical challenges. *Nat Med*. 2006;12(8):895-904. doi:10.1038/nm1469

33. Cañellas-Socias A, Cortina C, Hernando-Momblona X, et al. Metastatic recurrence in colorectal cancer arises from residual EMP1+ cells. *Nature*. 2022;611(7936):603-613. doi:10.1038/s41586-022-05402-9
34. Riihimäki M, Hemminki A, Sundquist J, Hemminki K. Patterns of metastasis in colon and rectal cancer. *Sci Rep*. 2016;6(1):29765. doi:10.1038/srep29765
35. Müller S, Köhler F, Hendricks A, et al. Brain Metastases from Colorectal Cancer: A Systematic Review of the Literature and Meta-Analysis to Establish a Guideline for Daily Treatment. *Cancers (Basel)*. 2021;13(4):900. doi:10.3390/cancers13040900
36. Rodriguez LG, Wu X, Guan JL. Wound-Healing Assay. In: *Cell Migration*. Humana Press; :023-030. doi:10.1385/1-59259-860-9:023
37. Chen HC. Boyden Chamber Assay. In: *Cell Migration*. Humana Press; :015-022. doi:10.1385/1-59259-860-9:015
38. Vinci M, Box C, Eccles SA. Three-Dimensional (3D) Tumor Spheroid Invasion Assay. *Journal of Visualized Experiments*. 2015;(99). doi:10.3791/52686
39. Sayed IM, El-Hafeez AAA, Maity PP, Das S, Ghosh P. Modeling colorectal cancers using multidimensional organoids. In: ; 2021:345-383. doi:10.1016/bs.acr.2021.02.005
40. Drost J, Clevers H. Organoids in cancer research. *Nat Rev Cancer*. 2018;18(7):407-418. doi:10.1038/s41568-018-0007-6
41. Fan H, Demirci U, Chen P. Emerging organoid models: leaping forward in cancer research. *J Hematol Oncol*. 2019;12(1):142. doi:10.1186/s13045-019-0832-4
42. Yang H, Sun L, Liu M, Mao Y. Patient-derived organoids: a promising model for personalized cancer treatment. *Gastroenterol Rep (Oxf)*. 2018;6(4):243-245. doi:10.1093/gastro/goy040
43. Barbáchano A, Fernández-Barral A, Bustamante-Madrid P, et al. Organoids and Colorectal Cancer. *Cancers (Basel)*. 2021;13(11):2657. doi:10.3390/cancers13112657
44. Sato T, Vries RG, Snippert HJ, et al. Single Lgr5 stem cells build crypt-villus structures in vitro without a mesenchymal niche. *Nature*. 2009;459(7244):262-265. doi:10.1038/nature07935
45. Goldhammer N, Kim J, Timmermans-Wielenga V, Petersen OW. Characterization of organoid cultured human breast cancer. *Breast Cancer Research*. 2019;21(1):141. doi:10.1186/s13058-019-1233-x

46. Lancaster MA, Renner M, Martin CA, et al. Cerebral organoids model human brain development and microcephaly. *Nature*. 2013;501(7467):373-379. doi:10.1038/nature12517
47. Jacob F, Salinas RD, Zhang DY, et al. A Patient-Derived Glioblastoma Organoid Model and Biobank Recapitulates Inter- and Intra-tumoral Heterogeneity. *Cell*. 2020;180(1):188-204.e22. doi:10.1016/j.cell.2019.11.036
48. Nuciforo S, Fofana I, Matter MS, et al. Organoid Models of Human Liver Cancers Derived from Tumor Needle Biopsies. *Cell Rep*. 2018;24(5):1363-1376. doi:10.1016/j.celrep.2018.07.001
49. Miller AJ, Dye BR, Ferrer-Torres D, et al. Generation of lung organoids from human pluripotent stem cells in vitro. *Nat Protoc*. 2019;14(2):518-540. doi:10.1038/s41596-018-0104-8
50. Tsai S, McOlash L, Palen K, et al. Development of primary human pancreatic cancer organoids, matched stromal and immune cells and 3D tumor microenvironment models. *BMC Cancer*. 2018;18(1):335. doi:10.1186/s12885-018-4238-4
51. Bartfeld S, Bayram T, van de Wetering M, et al. In Vitro Expansion of Human Gastric Epithelial Stem Cells and Their Responses to Bacterial Infection. *Gastroenterology*. 2015;148(1):126-136.e6. doi:10.1053/j.gastro.2014.09.042
52. Li X, Francies HE, Secrier M, et al. Organoid cultures recapitulate esophageal adenocarcinoma heterogeneity providing a model for clonality studies and precision therapeutics. *Nat Commun*. 2018;9(1):2983. doi:10.1038/s41467-018-05190-9
53. Turco MY, Gardner L, Hughes J, et al. Long-term, hormone-responsive organoid cultures of human endometrium in a chemically defined medium. *Nat Cell Biol*. 2017;19(5):568-577. doi:10.1038/ncb3516
54. Gao D, Vela I, Sboner A, et al. Organoid Cultures Derived from Patients with Advanced Prostate Cancer. *Cell*. 2014;159(1):176-187. doi:10.1016/j.cell.2014.08.016
55. Rauth S, Karmakar S, Batra SK, Ponnusamy MP. Recent advances in organoid development and applications in disease modeling. *Biochimica et Biophysica Acta (BBA) - Reviews on Cancer*. 2021;1875(2):188527. doi:10.1016/j.bbcan.2021.188527
56. Lo YH, Karlsson K, Kuo CJ. Applications of organoids for cancer biology and precision medicine. *Nat Cancer*. 2020;1(8):761-773. doi:10.1038/s43018-020-0102-y

57. HEK293 Cells: Background, Applications, Protocols, and More. https://www.synthego.com/hek293
58. Longo PA, Kavran JM, Kim MS, Leahy DJ. Transient Mammalian Cell Transfection with Polyethylenimine (PEI). In: ; 2013:227-240. doi:10.1016/B978-0-12-418687-3.00018-5
59. Lin SC, Haga K, Zeng XL, Estes MK. Generation of CRISPR–Cas9-mediated genetic knockout human intestinal tissue–derived enteroid lines by lentivirus transduction and single-cell cloning. *Nat Protoc*. 2022;17(4):1004-1027. doi:10.1038/s41596-021-00669-0
60. Davis HE, Morgan JR, Yarmush ML. Polybrene increases retrovirus gene transfer efficiency by enhancing receptor-independent virus adsorption on target cell membranes. *Biophys Chem*. 2002;97(2-3):159-172. doi:10.1016/S0301-4622(02)00057-1
61. Rio DC, Ares M, Hannon GJ, Nilsen TW. Purification of RNA Using TRIzol (TRI Reagent). *Cold Spring Harb Protoc*. 2010;2010(6):pdb.prot5439. doi:10.1101/pdb.prot5439
62. Ganesh K, Massagué J. Targeting metastatic cancer. *Nat Med*. 2021;27(1):34-44. doi:10.1038/s41591-020-01195-4
63. Kai F, Drain AP, Weaver VM. The Extracellular Matrix Modulates the Metastatic Journey. *Dev Cell*. 2019;49(3):332-346. doi:10.1016/j.devcel.2019.03.026
64. Bendardaf R, Buhmeida A, Ristamäki R, Syrjänen K, Pyrhönen S. MMP-1 (collagenase-1) expression in primary colorectal cancer and its metastases. *Scand J Gastroenterol*. 2007;42(12):1473-1478. doi:10.1080/00365520701485449
65. Dong W, Li H, Zhang Y, et al. Matrix metalloproteinase 2 promotes cell growth and invasion in colorectal cancer. *Acta Biochim Biophys Sin (Shanghai)*. 2011;43(11):840-848. doi:10.1093/abbs/gmr085
66. Sprangers J, Zaalberg IC, Maurice MM. Organoid-based modeling of intestinal development, regeneration, and repair. *Cell Death Differ*. 2021;28(1):95-107. doi:10.1038/s41418-020-00665-z
67. Kobayashi S, Ogasawara N, Watanabe S, et al. Collagen type I-mediated mechanotransduction controls epithelial cell fate conversion during intestinal inflammation. *Inflamm Regen*. 2022;42(1):49. doi:10.1186/s41232-022-00237-3

68. Sprangers J, Zaalberg IC, Maurice MM. Organoid-based modeling of intestinal development, regeneration, and repair. *Cell Death Differ*. 2021;28(1):95-107. doi:10.1038/s41418-020-00665-z
69. Henriksen K, Karsdal MA. Type I Collagen. In: *Biochemistry of Collagens, Laminins and Elastin*. Elsevier; 2016:1-11. doi:10.1016/B978-0-12-809847-9.00001-5
70. He X, Lee B, Jiang Y. Extracellular matrix in cancer progression and therapy. *Medical Review*. 2022;2(2):125-139. doi:10.1515/mr-2021-0028
71. Dekkers JF, Wiegerinck CL, de Jonge HR, et al. A functional CFTR assay using primary cystic fibrosis intestinal organoids. *Nat Med*. 2013;19(7):939-945. doi:10.1038/nm.3201
72. Tang XY, Xu L, Wang J, et al. DSCAM/PAK1 pathway suppression reverses neurogenesis deficits in iPSC-derived cerebral organoids from patients with Down syndrome. *Journal of Clinical Investigation*. 2021;131(12). doi:10.1172/JCI135763
73. Kim H, Park HJ, Choi H, et al. Modeling G2019S-LRRK2 Sporadic Parkinson's Disease in 3D Midbrain Organoids. *Stem Cell Reports*. 2019;12(3):518-531. doi:10.1016/j.stemcr.2019.01.020
74. Zhao J, Fu Y, Yamazaki Y, et al. APOE4 exacerbates synapse loss and neurodegeneration in Alzheimer's disease patient iPSC-derived cerebral organoids. *Nat Commun*. 2020;11(1):5540. doi:10.1038/s41467-020-19264-0
75. Garcez PP, Loiola EC, Madeiro da Costa R, et al. Zika virus impairs growth in human neurospheres and brain organoids. *Science (1979)*. 2016;352(6287):816-818. doi:10.1126/science.aaf6116
76. Zhao B, Ni C, Gao R, et al. Recapitulation of SARS-CoV-2 infection and cholangiocyte damage with human liver ductal organoids. *Protein Cell*. 2020;11(10):771-775. doi:10.1007/s13238-020-00718-6
77. Rae C, Amato F, Braconi C. Patient-Derived Organoids as a Model for Cancer Drug Discovery. *Int J Mol Sci*. 2021;22(7):3483. doi:10.3390/ijms22073483
78. Neal JT, Li X, Zhu J, et al. Organoid Modeling of the Tumor Immune Microenvironment. *Cell*. 2018;175(7):1972-1988.e16. doi:10.1016/j.cell.2018.11.021